Heavy flavor spectroscopy studies at ATLAS

Vincenzo Canale
Università di Napoli “Federico II” and INFN

LHCP2024: Boston 03/6-07/6

Outline

A. Introduction

1) Physics context
2) Experimental aspects (data, detector, trigger)

B. Narrow Low-mass resonances in the 4-muon final state

1) Decay chain, triggers and data samples
2) $\Upsilon(1s)+\mu^+\mu^- \rightarrow \mu^+\mu^- \mu^+\mu^-$ event selection and analysis
3) Statistical fits
4) Signal interpretation and limit setting

C. Di-charmonium Events in the 4-muon Final State

1) "2-J/ψ $\rightarrow$ 4μ" and "J/ψ +ψ(2s) $\rightarrow$ 4μ" selection
2) Background studies
3) Analysis Results

D. Conclusions

A) Introduction

A.1 Physics context

→ since the discovery of X(3872) in 2003 the exciting era of the un-conventional hadronic physics has started with an increasing evidence of new tetra-quarks (TQ) and penta-quark (PQ) states (e.g. X, Y, Z,…) which triggered a very large number of theoretical investigations on the behaviour of the strong interactions.

A) Introduction

A.1 Physics context

→ since the discovery of X(3872) in 2003 the exciting era of the un-conventional hadronic physics has started with an increasing evidence of new tetra-quarks (TQ) and penta-quark (PQ) states (e.g. X, Y, Z,…) which triggered a very large number of theoretical investigations on the behaviour of the strong interactions.

→ heavy quark masses strongly suppress Q-Qbar production from vacuum then the presence of heavy flavour doublets (Q-Qbar) in the final states is an excellent hint for searching and interpreting these exotic states like $T_{(QQbarQQbar)}$.

→ in addition, several extensions of the SM foresee the presence of new particles decaying to four leptons via mechanisms involving quarkonium final states

A) Introduction

A.1 Physics context

→ since the discovery of X(3872) in 2003 the exciting era of the un-conventional hadronic physics has started with an increasing evidence of new tetra-quarks (TQ) and penta-quark (PQ) states (e.g. X, Y, Z,…) which triggered a very large number of theoretical investigations on the behaviour of the strong interactions.

→ heavy quark masses strongly suppress Q-Qbar production from vacuum then the presence of heavy flavour doublets (Q-Qbar) in the final states is an excellent hint for searching and interpreting these exotic states like $T_{(QQbarQQbar)}$.

→ in addition, several extensions of the SM foresee the presence of new particles decaying to four leptons via mechanisms involving quarkonium final states

→ the experimental signature of heavy quarkonia is certainly more effective in the LHC complex environment via well identifiable physics state (e.g. $J/\psi \rightarrow \mu\mu$, $Y(1s) \rightarrow \mu\mu$)

→ ATLAS studied four muon final states in pp collisions with energies 8-13 TeV, via quarkonia final states and different invariant mass ranges

A.2 Experimental aspects

Run I: 21.3 fb^{-1} at 8 TeV (2012)
Run II: 140 fb^{-1} at 13 TeV (2015-2018)

A.2.1 Data samples

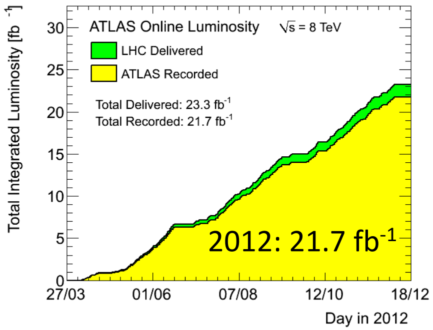

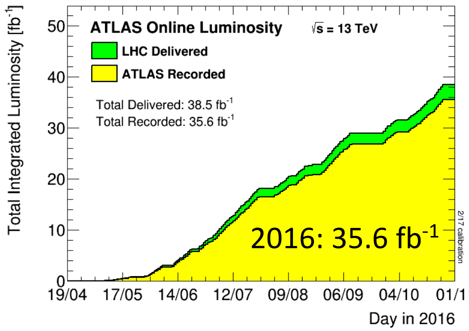

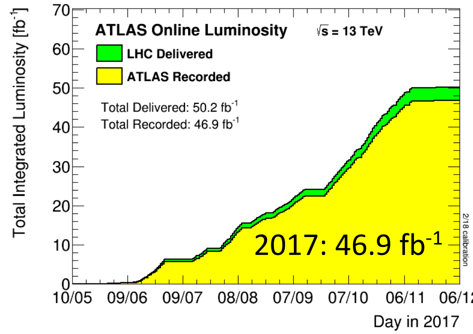

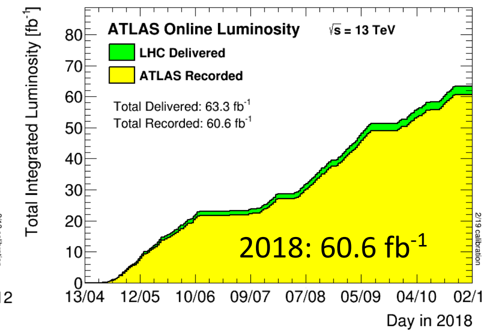

→ Difficulty in combining different energies and beam conditions (e.g. background)

A.2 Experimental aspects

Run I: 21.3 fb^{-1} at 8 TeV (2012)
Run II: 140 fb^{-1} at 13 TeV (2015-2018)

A.2.1 Data samples

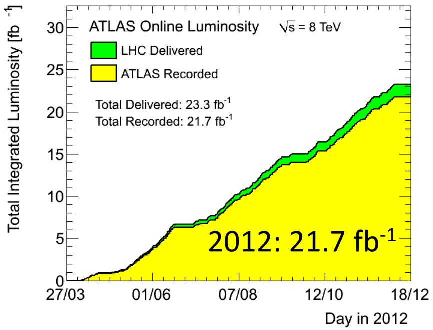

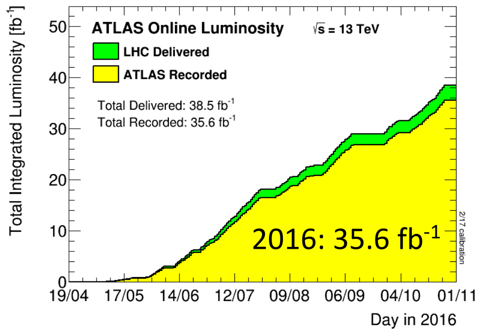

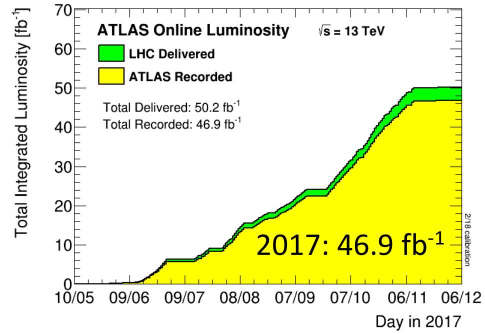

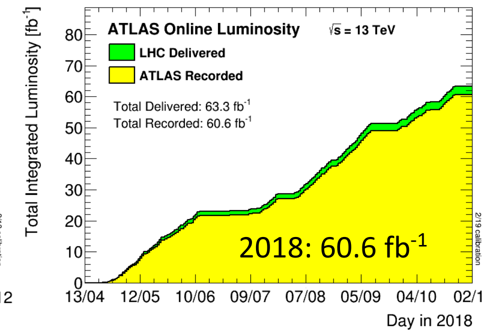

→ Difficulty in combining different energies and beam conditions (e.g. background)

A.2.2 Detector and trigger

Inner Det.→ $|\eta|<2.5$, $\sigma_{Pt}/p_t \approx 0{,}0004\ p_t\,(\text{GeV}) + 0{,}015$

Muon Sys.→ $|\eta|<2.7$→ $\sigma_{Pt}/p_t \leq 0.1$ up to 1 TeV

$\langle B_{tor}\rangle = 0{,}5$ T $\quad B_{sol} = 2$ T

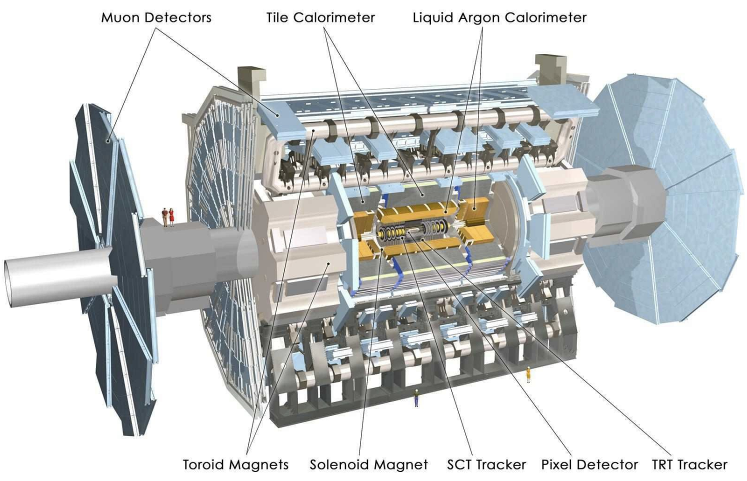

A.2 Experimental aspects

Run I: 21.3 fb^{-1} at 8 TeV (2012)
Run II: 140 fb^{-1} at 13 TeV (2015-2018)

A.2.1 Data samples

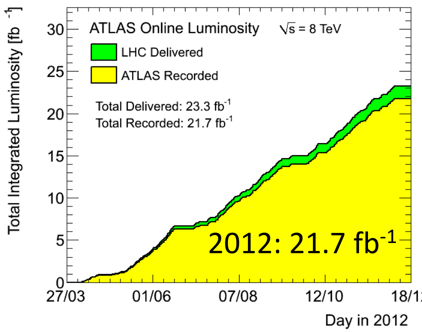

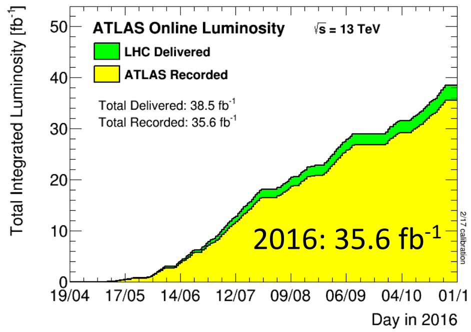

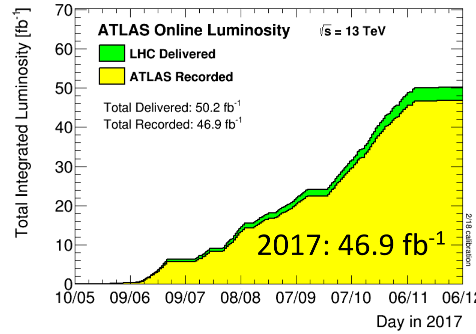

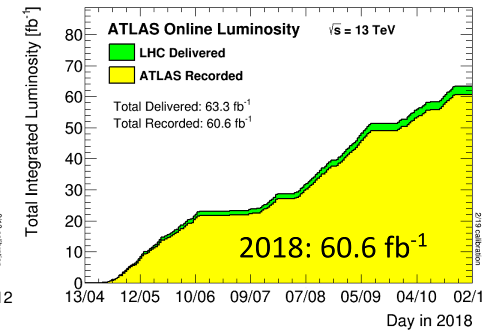

→ Difficulty in combining different energies and beam conditions (e.g. background)

A.2.2 Detector and trigger

Inner Det.→ $|\eta|<2.5$, $\sigma_{Pt}/p_t \approx 0{,}0004\, p_t\,(\text{GeV}) + 0{,}015$
Muon Sys.→ $|\eta|<2.7$→ $\sigma_{Pt}/p_t \leq 0.1$ up to 1 TeV

$\langle B_{tor}\rangle=0{,}5$ T $B_{sol}=2$ T

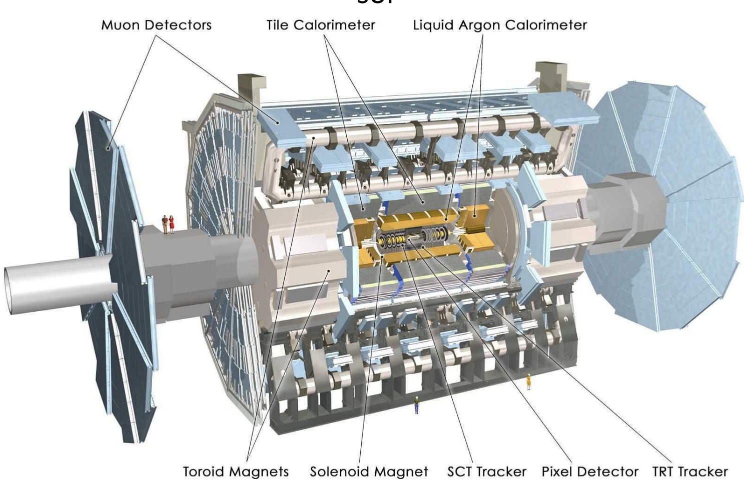

L1 Muon trigger with thresholds: Pt > 4, 6 GeV and multiplicity requirement

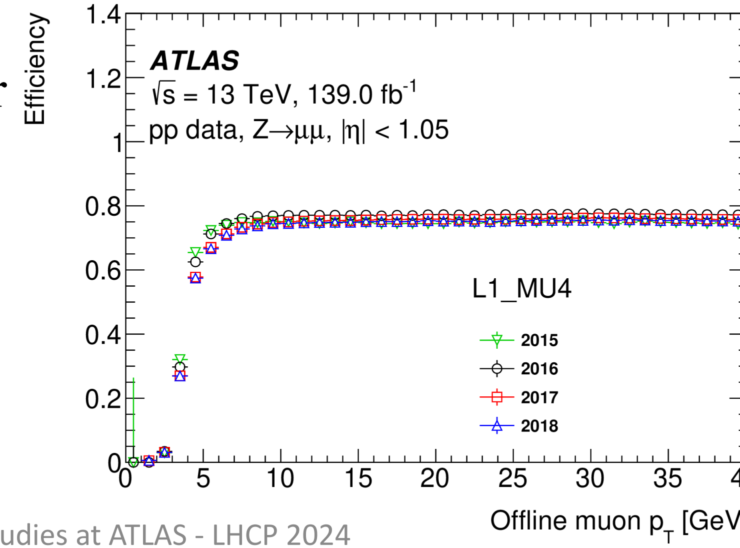

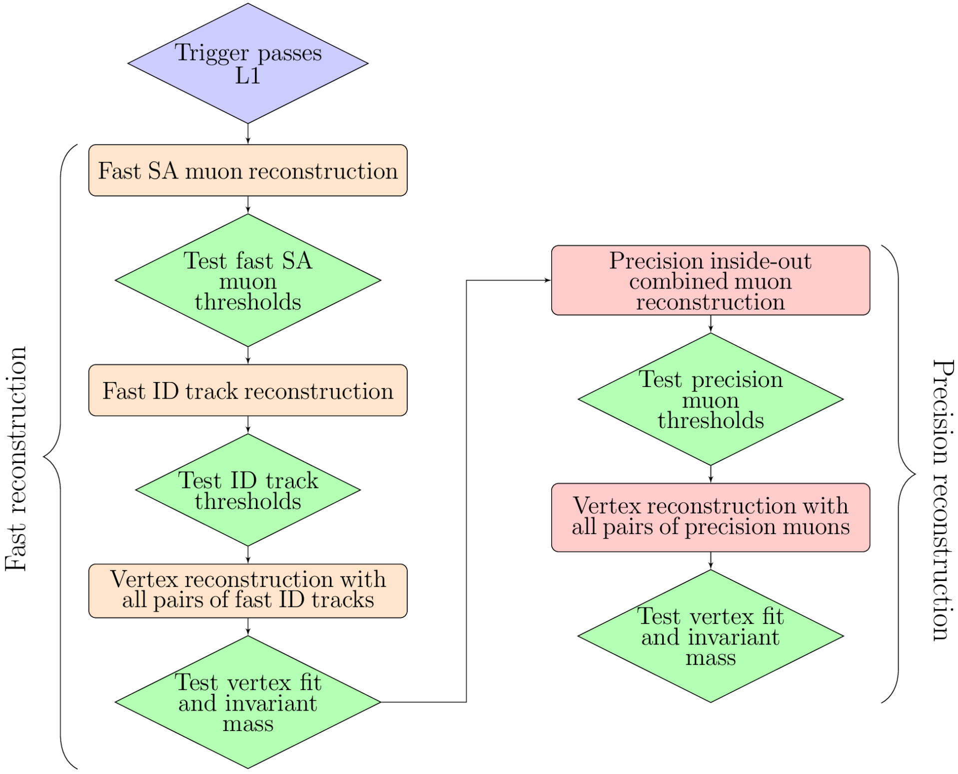

HL-muon trigger for BLS physics (vertex and mass constraints) after L1:

- fast reconstruction with ID
- precision reconstruction: topology, vertices and invariant mass;
- dedicated requirements for specific channels (e.g. 2μ, 3μ, J/ψ–>μμ, Y–>μμ, B–> μμ, ….)

HL-muon trigger for BLS physics (vertex and mass constraints) after L1:

- fast reconstruction with ID
- precision reconstruction: topology, vertices and invariant mass;
- dedicated requirements for specific channels (e.g. 2μ, 3μ, J/ψ–>μμ, Y–>μμ, B–> μμ, ….)

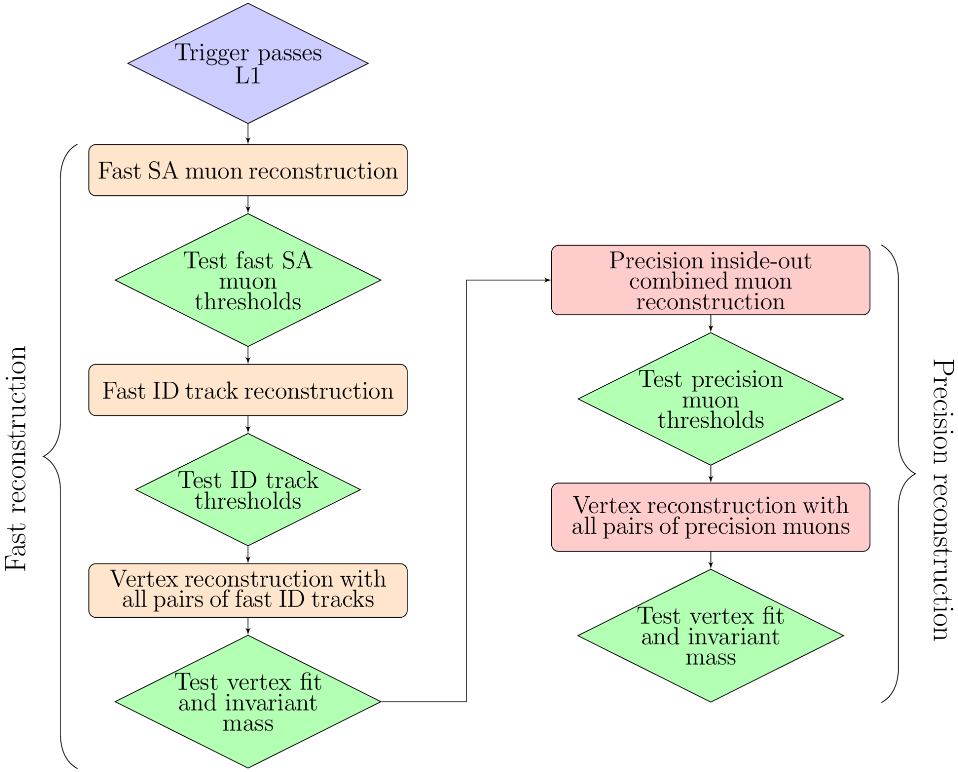

Muon reconstruction performance

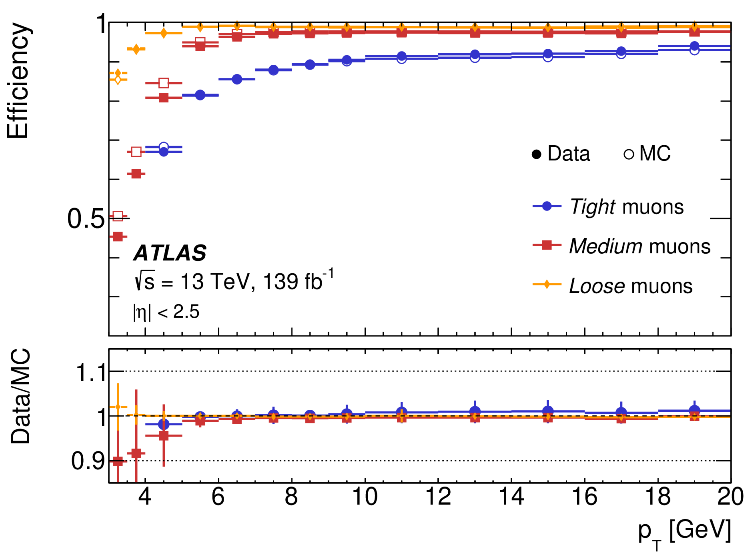

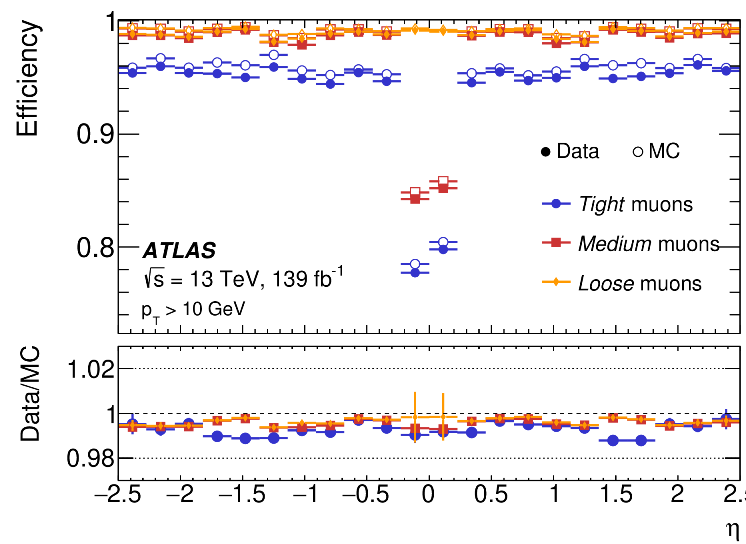

Working point	$3 < p_T$ [GeV] < 5		$5 < p_T$ [GeV] < 20	
	ϵ_μ [%]	ϵ_{had} [%]	ϵ_μ [%]	ϵ_{had} [%]
Loose	90	1.17	98	1.06
Medium	70	0.63	97	0.85
Tight	36	0.15	90	0.38

B. Narrow Low-mass resonances in 4-muon final state

ATLAS-CONF-2023-041

B.1 Signature, triggers and data samples

Signature: to optimize both the physics interest (e.g tetraquarks or scalar/pseudoscalar Higgs like particles) and the experimental signature, the search is performed via the 4-muon final state from the decay chain $X \rightarrow Y(1s)+\mu^{+}\mu^{-} \rightarrow \mu^{+}\mu^{-}\mu^{+}\mu^{-}$ in the range $m_{4\mu}$ [10-50] GeV

B. Narrow Low-mass resonances in 4-muon final state

ATLAS-CONF-2023-041

B.1 Signature, triggers and data samples

Signature: to optimize both the physics interest (e.g tetraquarks or scalar/pseudoscalar Higgs like particles) and the experimental signature, the search is performed via the 4-muon final state from the decay chain X→Y(1s)+$\mu^+\mu^-$ → $\mu^+\mu^-$ $\mu^+\mu^-$ in the range $m_{4\mu}$ [10-50] GeV

Trigger requires: more than 2 or 3 muons with p_t>4 GeV, muon pair opposite charge and mass range for $m_{\mu\mu}$, but with different configurations:

- 8 Tev (2012) combination of un-prescaled 2-μ and 3-μ → L=20.3 fb^{-1}
- 13 TeV (2015-2017) pre-scaled 3-μ → L=51.5 fb^{-1}
- 13 TeV(2018) restricted 3μ, pair opposite charge and $m_{\mu\mu}$in [8-12]GeV→L=58.5 fb^{-1}

B. Narrow Low-mass resonances in 4-muon final state

ATLAS-CONF-2023-041

B.1 Signature, triggers and data samples

Signature: to optimize both the physics interest (e.g tetraquarks or scalar/pseudoscalar Higgs like particles) and the experimental signature, the search is performed via the 4-muon final state from the decay chain $X \rightarrow Y(1s) + \mu^+\mu^- \rightarrow \mu^+\mu^- \mu^+\mu^-$ in the range $m_{4\mu}$ [10-50] GeV

Trigger requires: more than 2 or 3 muons with $p_t > 4$ GeV, muon pair opposite charge and mass range for $m_{\mu\mu}$, but with different configurations:

- 8 Tev (2012) combination of un-prescaled 2-μ and 3-μ → $L = 20.3\ fb^{-1}$
- 13 TeV (2015-2017) pre-scaled 3-μ → $L = 51.5\ fb^{-1}$
- 13 TeV(2018) restricted 3μ, pair opposite charge and $m_{\mu\mu}$ in [8-12]GeV → $L = 58.5\ fb^{-1}$

Reconstruction in "same" conditions and with the same software:

- for signal, MC generators of tetraquarks models or Higgs-like $X \rightarrow Y(1s) + \mu^+\mu^-$ are used solely for interpretation
- for background MC generators of several standard processes (e.g b-b-*bar*, c-c-*bar*, W, Z/γ*, ..) producing muons or from misidentification of others charged particles
- events are passed through simulation of ATLAS and pile-up is taken into account

B.2 $\Upsilon(1s)+\mu^+\mu^- \rightarrow \mu^+\mu^- \mu^+\mu^-$ event selection and analysis

B.2.1 Event reconstruction

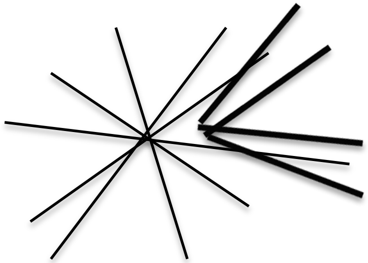

1 μ–quadruplet

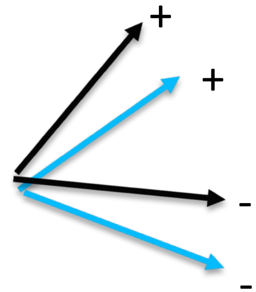

2 μ–doublets with opposite charge OS

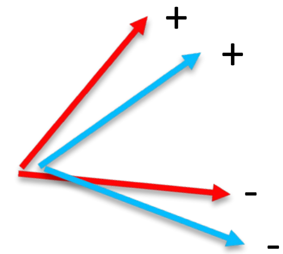

$\Upsilon \rightarrow \mu^+\mu^-$ + OS doublet

Candidate object	Requirements
Muons	$p_T(\mu) > 3$ GeV and $\|\eta\| < 2.5$, $\|z_0 \sin\theta\| < 1$ mm and $\|d_0/\sigma_{d_0}\| < 6$
Muon quadruplet	≥ 3 muons passing LowPt selection criteria, $\sum q_\mu = 0$, four-muon vertex fit $\chi^2/N_{d.o.f} \leq 10$,
Muon doublet	di-muon vertex fit $\chi^2 < 3$
$\Upsilon(1S)$ candidate	OS muon doublet with $p_T(\mu_{1,2}) > 4$ GeV, 9.2 GeV $\leq m_{\mu^+\mu^-} \leq$ 9.7 GeV
$\Upsilon(1S) + \mu^+\mu^-$ candidate events	$\Upsilon(1S)$ candidate plus OS muon doublet with $m_{\mu^+\mu^-} > 1$ GeV, both muon doublets point to a common PV

B.2.2 Analysis of 8 TeV data

Obtain the $m_{4\mu}$-distribution for (Υ(1s) + OS)

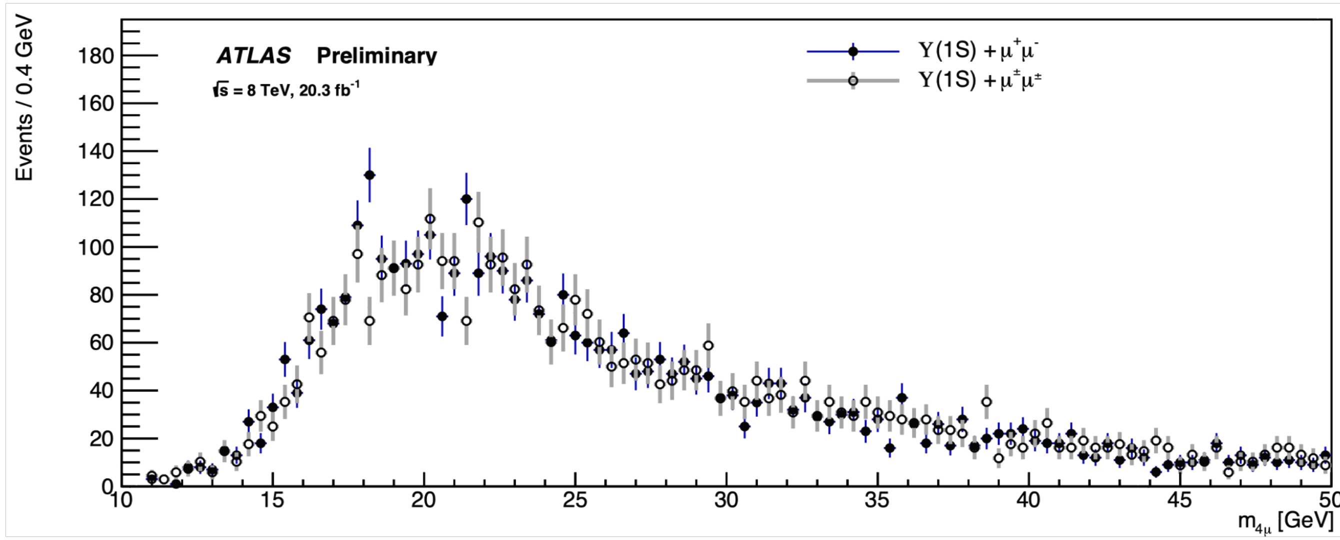

B.2.2 Analysis of 8 TeV data

Obtain the $m_{4\mu}$-distribution for (Υ(1s) + OS) → excess around 18 and 21 GeV

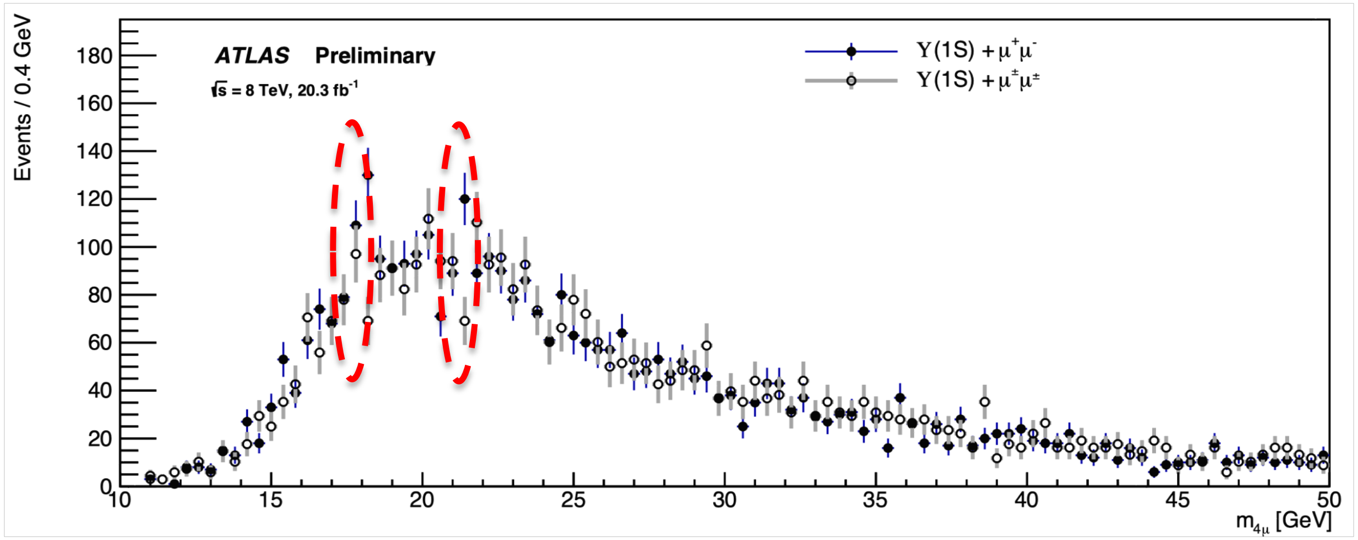

B.2.2 Analysis of 8 TeV data

Obtain the $m_{4\mu}$-distribution for (Y(1s) + OS) → excess around 18 and 21 GeV

No blinded analysis then extensive study for the validation:

→ (Y(1s) + SS) to test the global shape

→ MC studies with (Y(1s)+2-trks),(1μ+3-trks) removing muon-ID criteria

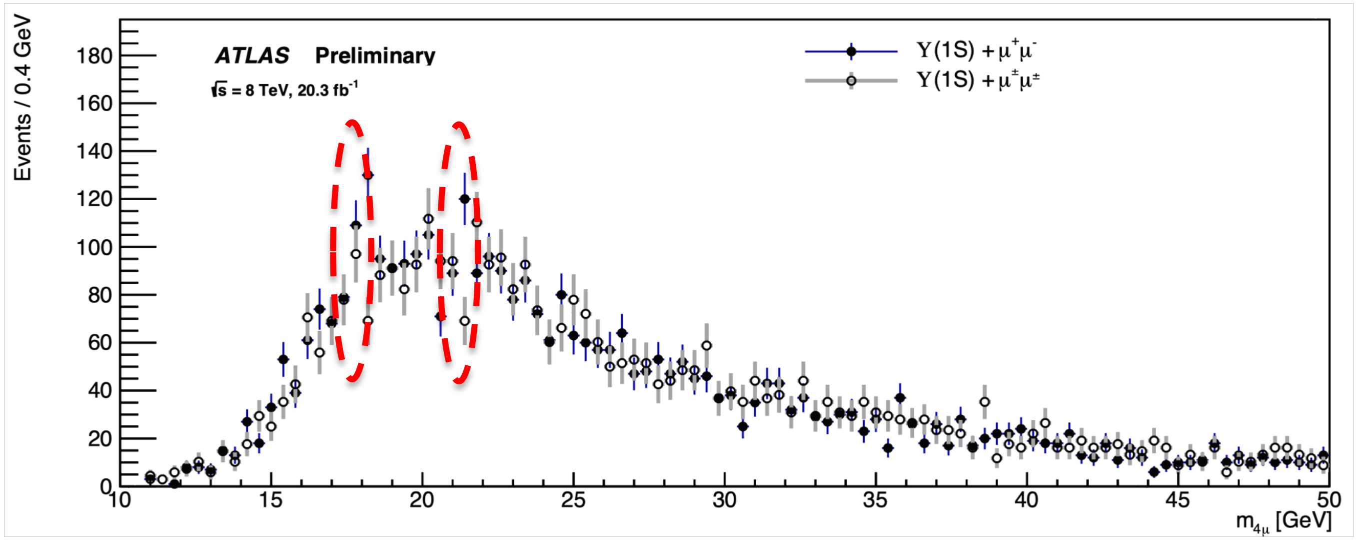

B.2.2 Analysis of 8 TeV data

Obtain the $m_{4\mu}$-distribution for (Υ(1s) + OS) → excess around 18 and 21 GeV

No blinded analysis then extensive study for the validation:

→ (Υ(1s) + SS) to test the global shape

→ MC studies with (Υ(1s)+2-trks),(1μ+3-trks) removing muon-ID criteria

→ events from Υ(1s) side-bands:[8.5,9.0] and [11.0,11.5] GeV

→ mixing of muon doublets from different pp collisions in quadruplet

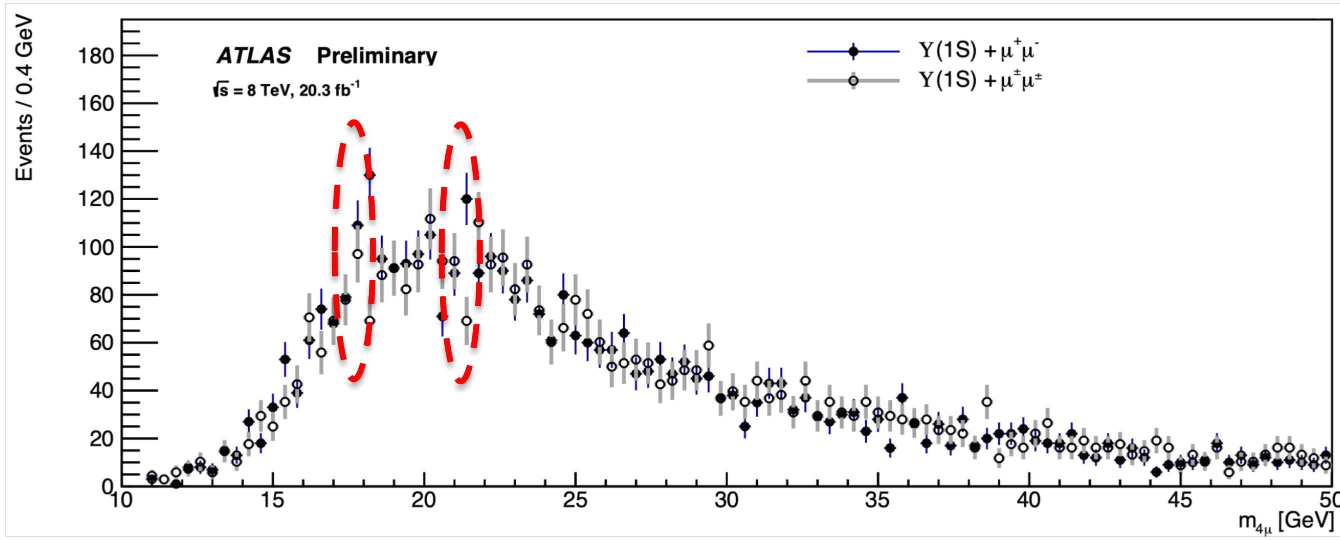

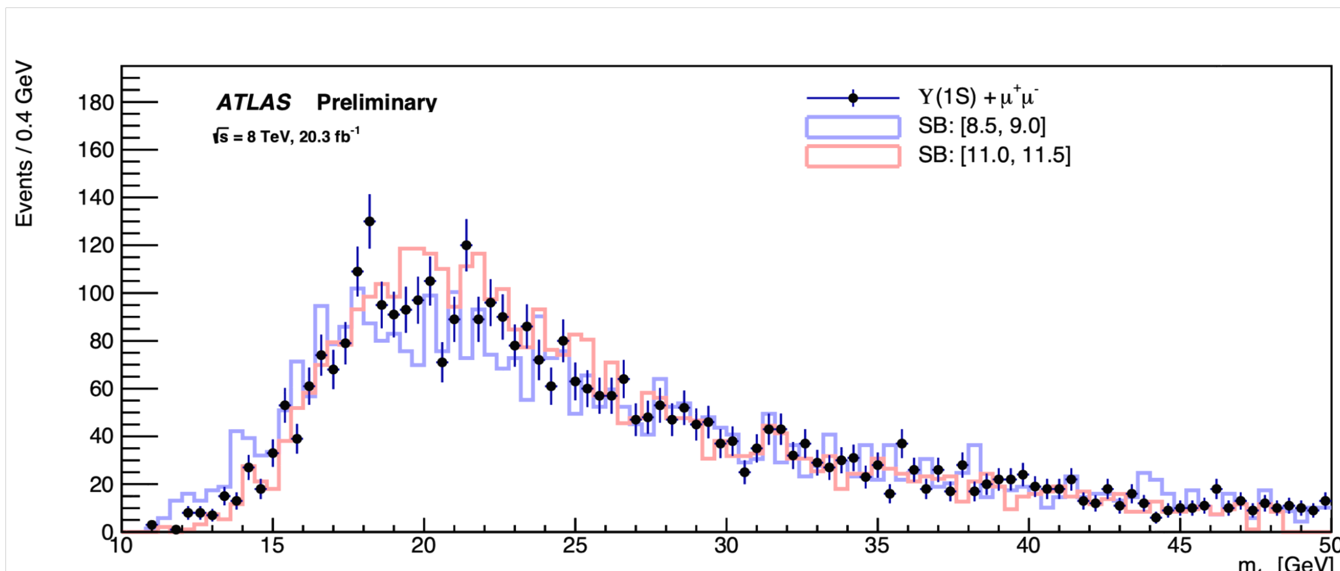

→ No evidence for manufactured peaks in $m_{4\mu}$-distribution

B.2.3 Analysis of 13 TeV data

Data at 13 TeV allow an independent cross check but due to trigger differences
→ two separated samples for (2015-2017) and 2018 data

B.2.3 Analysis of 13 TeV data

Data at 13 TeV allow an independent cross check but due to trigger differences
→ two separated samples for (2015-2017) and 2018 data

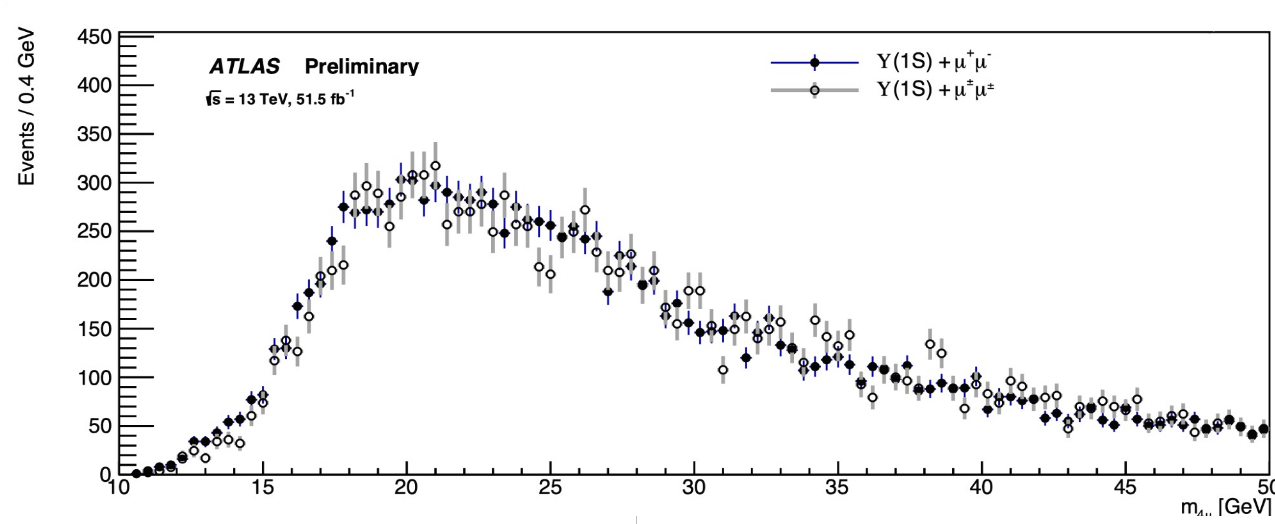

→ same selection, get the (Y(1s)+OS) and (Y(1s) + SS) $m_{4\mu}$-distributions
→ physics conditions at 13 TeV enhance combinatorial background;

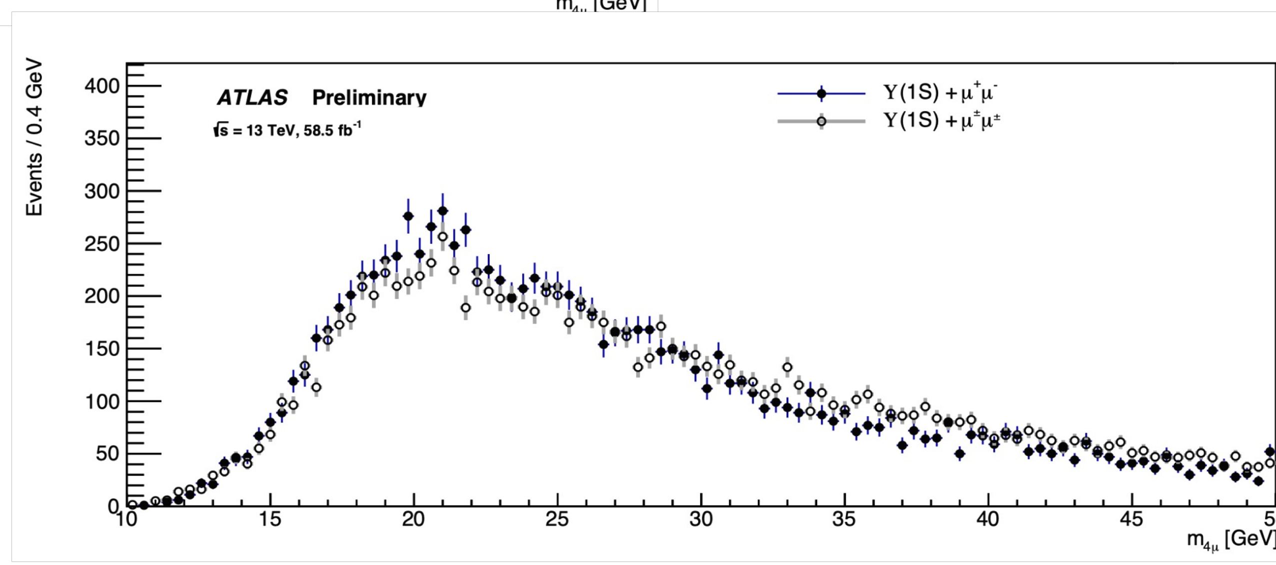

B.2.3 Analysis of 13 TeV data

Data at 13 TeV allow an independent cross check but due to trigger differences
→ two separated samples for (2015-2017) and 2018 data

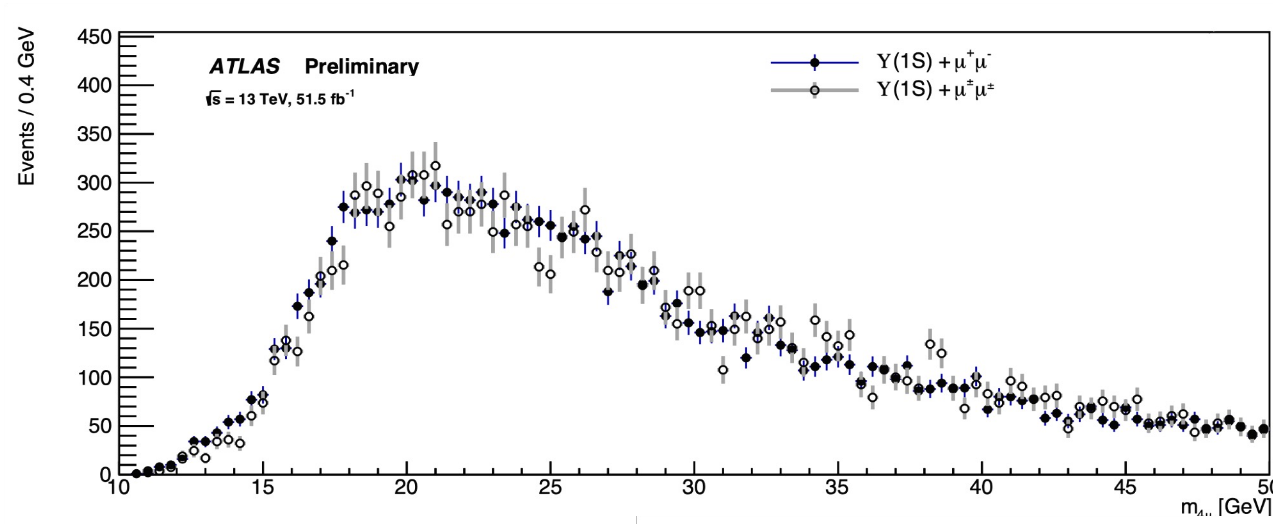

→ same selection, get the (Υ(1s)+OS) and (Υ(1s) + SS) $m_{4\mu}$-distributions
→ physics conditions at 13 TeV enhance combinatorial background;

-for (2015-2017) shape is ok
-for 2018 OS enhancement due to the opposite sign in 3-μ trigger

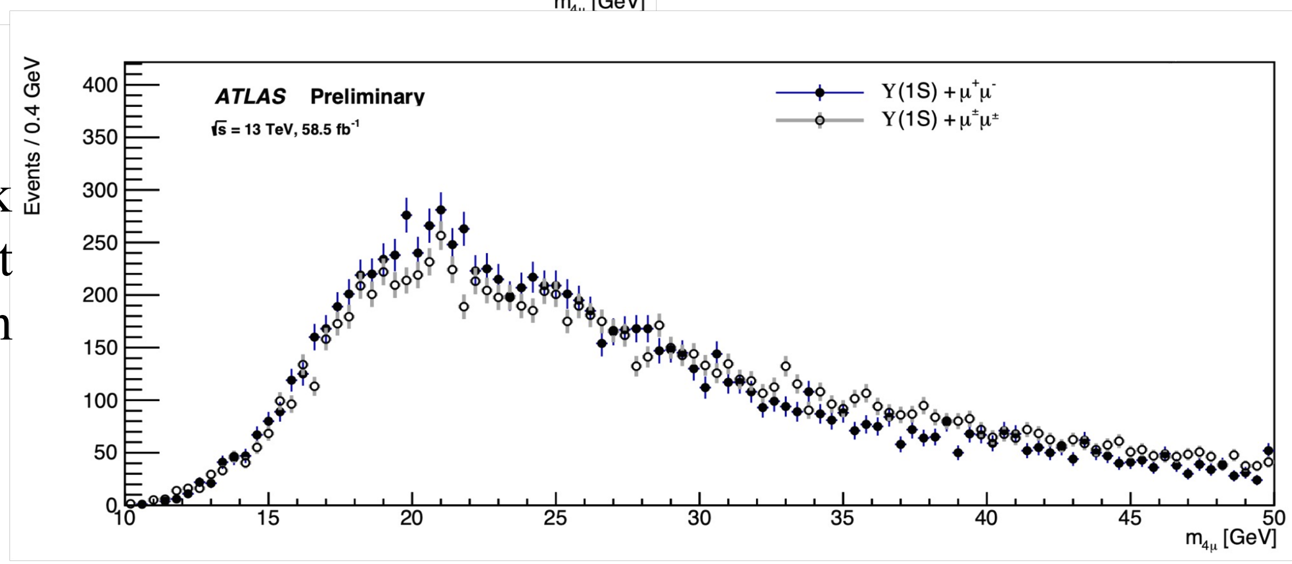

→ no excess is observed around 18 and 21 GeV

B.3 Statistical fits Perform unbinned maximum likelihood fit to $m_{4\mu}$-distribution

$$L(N_S, m_X, \sigma_X, \vec{\theta}) = \prod_{n \text{ events}} \left[N_B \cdot f_B(m_{4\mu}; \vec{\theta}_{\mathrm{B}}) + N_S \cdot f_S(m_{4\mu}; m_X, \sigma_X, \vec{\theta}_{\mathrm{S}}) \right] \cdot \frac{e^{-(N_B+N_S)}(N_B+N_S)^n}{n!}.$$

-m_X resonance mass, σ_X width (~200 MeV), N_S (N_B) number of signal (background)

-f_S signal pdf from simulation → good description with Gaussian or DSCB

-f_B background pdf → from (Y(1s) + SS) in $\Delta m_{4\mu}$ windows with 4-order C-polynom.

→ fits sliding $\Delta m_{4\mu}$=10 GeV around m_X between 15-45 GeV at step δm_X=0.05GeV

B.3 Statistical fits Perform unbinned maximum likelihood fit to $m_{4\mu}$-distribution

$$L(N_S, m_X, \sigma_X, \vec{\theta}) = \prod_{n \text{ events}} \left[N_B \cdot f_B(m_{4\mu}; \vec{\theta}_\mathrm{B}) + N_S \cdot f_S(m_{4\mu}; m_X, \sigma_X, \vec{\theta}_\mathrm{S}) \right] \cdot \frac{e^{-(N_B+N_S)}(N_B+N_S)^n}{n!}.$$

- m_X resonance mass, σ_X width (~200 MeV), N_S (N_B) number of signal (background)
- f_S signal pdf from simulation → good description with Gaussian or DSCB
- f_B background pdf → from (Y(1s) + SS) in $\Delta m_{4\mu}$ windows with 4-order C-polynom.

→ fits sliding $\Delta m_{4\mu}$=10 GeV around m_X between 15-45 GeV at step δm_X=0.05GeV

B.3.1 Results for 8 TeV data

$$q_0(m_X, \sigma_X) = -2\ln\left(\frac{L(0, m_X, \sigma_X, \hat{\hat{\vec{\theta}}})}{L(\hat{N}_S, m_X, \sigma_X, \hat{\vec{\theta}})} \right)$$

The local p-value with profile likelihood ratio statistics and asymptotic approximation and global significance with look elsewhere effect.

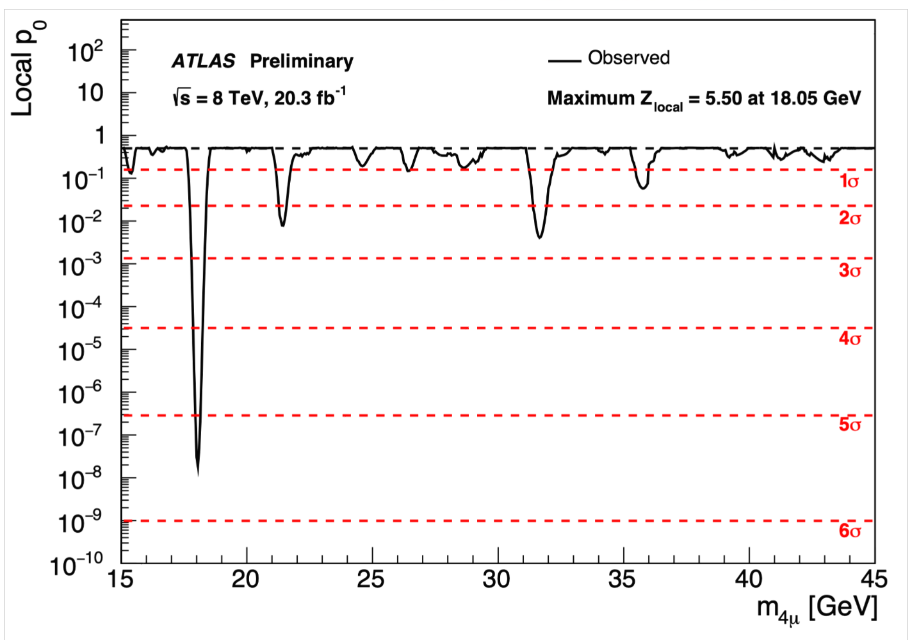

→ smallest p-value at m_X~18.5 GeV with significance 5.5σ (4.6σ global), the other minima (21 and 31 GeV) are incompatible with physical resonance (width<<resolution)

B.3 Statistical fits

Perform unbinned maximum likelihood fit to $m_{4\mu}$-distribution

$$L(N_S, m_X, \sigma_X, \vec{\theta}) = \prod_{n \text{ events}} \left[N_B \cdot f_B(m_{4\mu}; \vec{\theta}_B) + N_S \cdot f_S(m_{4\mu}; m_X, \sigma_X, \vec{\theta}_S) \right] \cdot \frac{e^{-(N_B+N_S)} (N_B+N_S)^n}{n!}.$$

- m_X resonance mass, σ_X width (~200 MeV), N_S (N_B) number of signal (background)
- f_S signal pdf from simulation → good description with Gaussian or DSCB
- f_B background pdf → from (Y(1s) + SS) in $\Delta m_{4\mu}$ windows with 4-order C-polynom.

→ fits sliding $\Delta m_{4\mu}$=10 GeV around m_X between 15-45 GeV at step δm_X=0.05GeV

B.3.1 Results for 8 TeV data

$$q_0(m_X, \sigma_X) = -2 \ln \left(\frac{L(0, m_X, \sigma_X, \hat{\hat{\theta}})}{L(\hat{N}_S, m_X, \sigma_X, \hat{\theta})} \right)$$

The local p-value with profile likelihood ratio statistics and asymptotic approximation and global significance with look elsewhere effect.

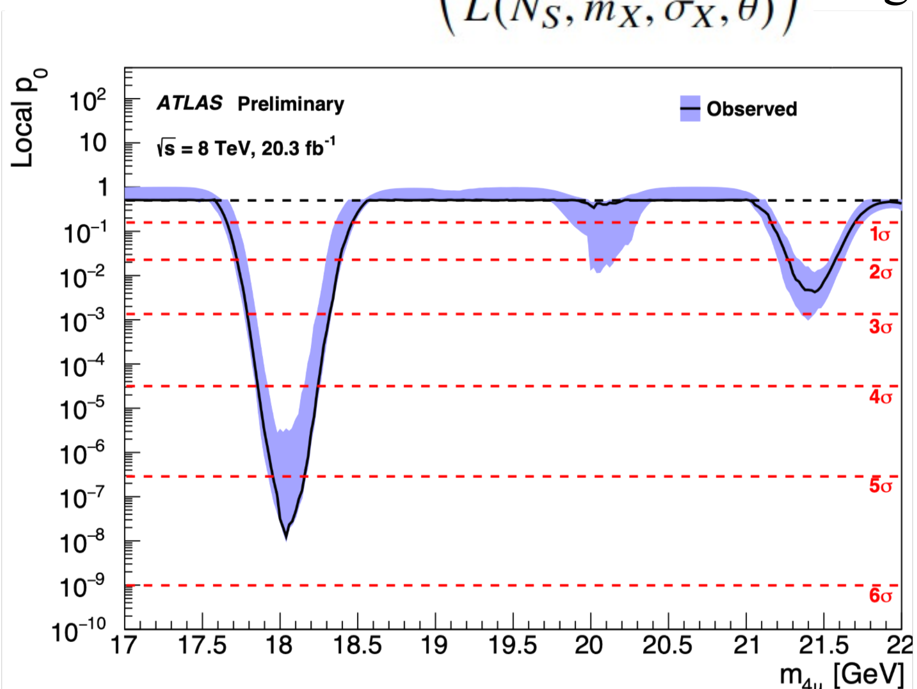

→ smallest p-value at m_X~18.5 GeV with significance 5.5σ (4.6σ global), the other minima (21 and 31 GeV) are incompatible with physical resonance (width<<resolution)

→ impact of variation of background parametrization 3/5-order C-polynomial

→ impact of the fit range $\Delta m_{4\mu}$= 6–12 GeV, for m_X=18.5 GeV significance change from 4.5σ to 5.6σ

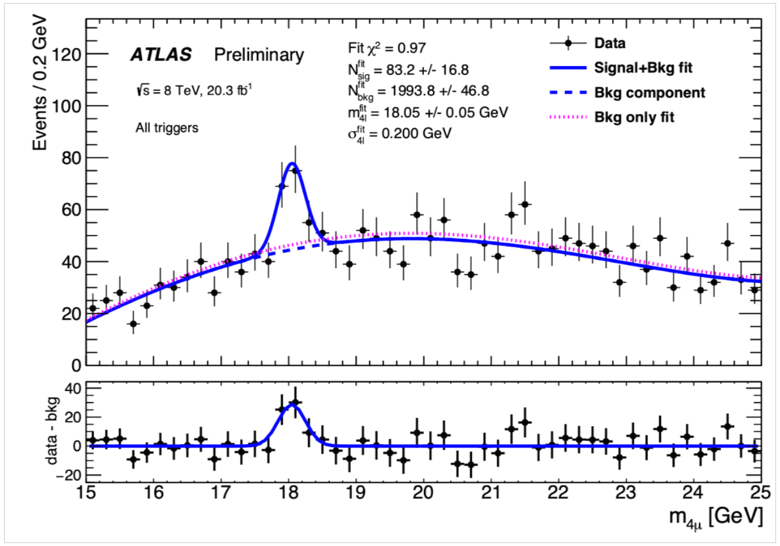

Baseline fit in the range $m_{4\mu}$:[15–25] GeV

m_X=(18.05+/-0.05)GeV

N_S= 83 +/- 17

N_B= 1994 +/- 47

σ_X= 200 MeV

χ^2_{dof}= 0.97

→no estimation of systematic uncertainties

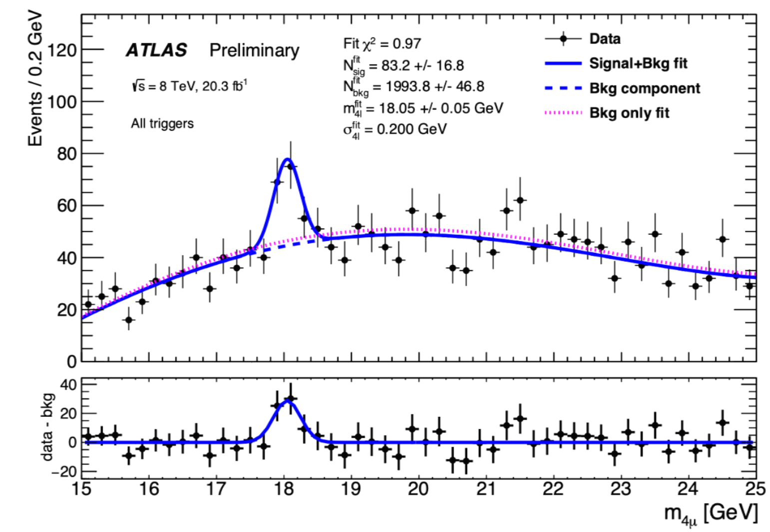

Baseline fit in the range $m_{4\mu}$:[15–25] GeV
m_X=(18.05+/-0.05)GeV
N_S= 83 +/- 17
N_B= 1994 +/- 47
σ_X= 200 MeV
χ^2_{dof}= 0.97
→no estimation of systematic uncertainties

An extensive study of cut-variations in the different steps of the analysis, with respect to the baseline, has been carried to test the stability of the apparent excess.

In terms of significance the excursion was between:

- local: 3.6σ ←→ 6.3σ
- global: 1.9σ ←→ 5.4σ

Selection criteria	N_B	Mass (GeV)	N_S	Significance (σ)
Baseline	1994 ± 47	18.05 ± 0.05	83 ± 17	5.5
Selection variations from the baseline				
≥ 2 LowPt muons	3124 ± 59	18.09 ± 0.06	94 ± 20	5.0
= 4 LowPt muons	689 ± 28	18.03 ± 0.07	37 ± 10	4.1
$m^{\text{non-res}}_{\mu^+\mu^-} > 0$ GeV	2515 ± 53	18.00 ± 0.06	81 ± 19	4.7
$m^{\text{non-res}}_{\mu^+\mu^-} > 0.5$ GeV	2306 ± 51	18.00 ± 0.05	87 ± 18	5.3
$m^{\text{non-res}}_{\mu^+\mu^-} > 2$ GeV	1696 ± 43	18.05 ± 0.07	58 ± 15	4.3
Vertex fit $\chi^2/N_{\text{d.o.f}} \leq 4$	1705 ± 43	18.03 ± 0.05	69 ± 15	5.0
Vertex fit $\chi^2/N_{\text{d.o.f}} \leq 20$	2077 ± 48	18.04 ± 0.05	81 ± 17	5.0
$m_{\Upsilon(1S)} \pm 2\sigma_m$ window	3705 ± 64	18.09 ± 0.06	90 ± 22	4.5
$\Upsilon(1S)$ mass correction	1998 ± 47	18.02 ± 0.08	64 ± 17	4.1
$m^{\text{non-res}}_{\mu^+\mu^-} < m_{\Upsilon(1S)}$	1418 ± 40	18.06 ± 0.05	94 ± 17	6.3
$p_T > 2.5$ GeV non-res. muons	2741 ± 55	18.05 ± 0.05	70 ± 19	4.1
$p_T > 4$ GeV non-res. muons	982 ± 33	18.06 ± 0.08	35 ± 11	3.6
Tight IP cuts	1469 ± 40	18.01 ± 0.05	71 ± 15	5.5
Lifetime $\lvert\tau/\sigma_\tau\rvert < 3$	1873 ± 45	18.04 ± 0.05	86 ± 17	5.6
MBS < 3	1749 ± 44	18.05 ± 0.04	83 ± 16	5.8

B.3.2 Results for 13 TeV data

Data at 13 TeV provide independent and blinded sample to check the observed excess at m_X=18.05 GeV in 8 TeV → same selection is reproduced and $m_{4\mu}$ distribution is fitted in the range [15–25] GeV similarly to 8 TeV data:
→ no significant excess is observed

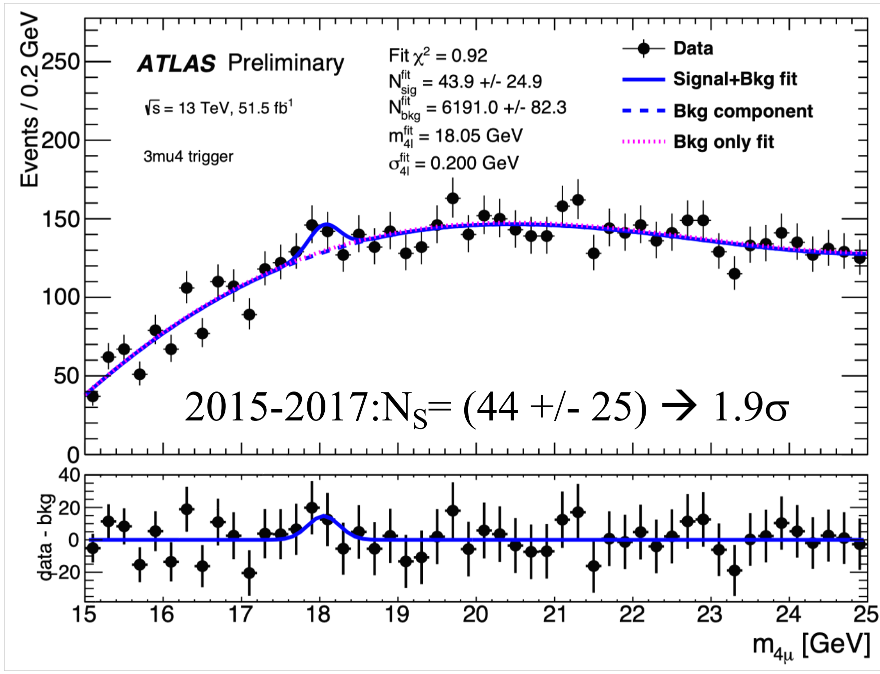

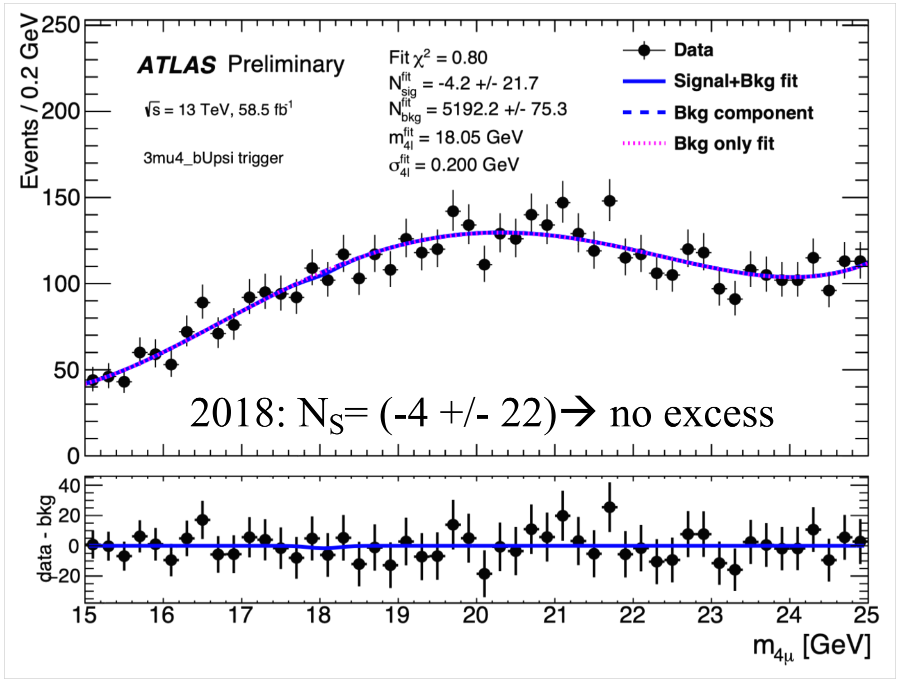

B.3.2 Results for 13 TeV data

Data at 13 TeV provide independent and blinded sample to check the observed excess at m_X=18.05 GeV in 8 TeV → same selection is reproduced and $m_{4\mu}$ distribution is fitted in the range [15–25] GeV similarly to 8 TeV data:
→ no significant excess is observed

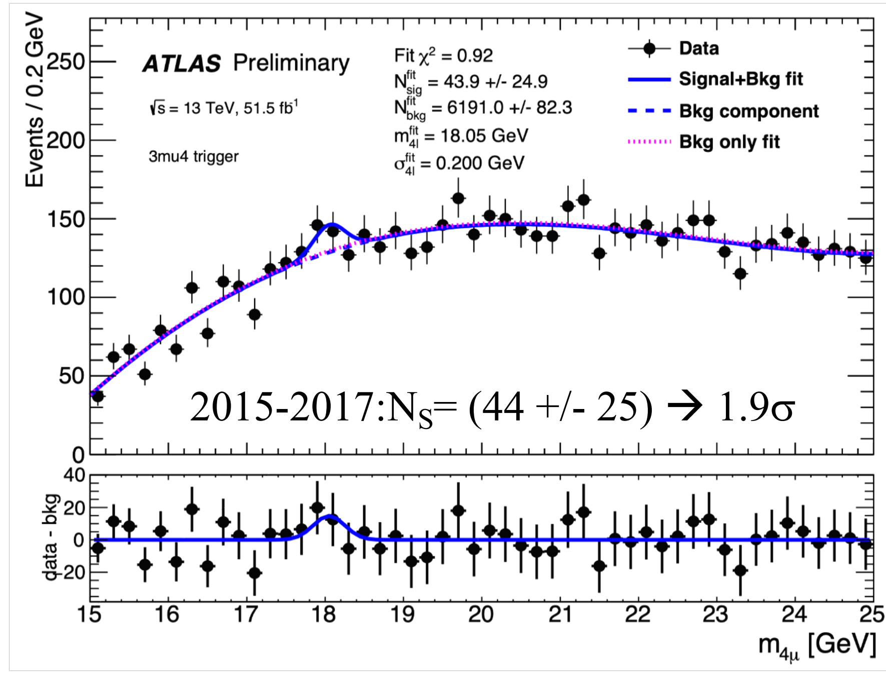

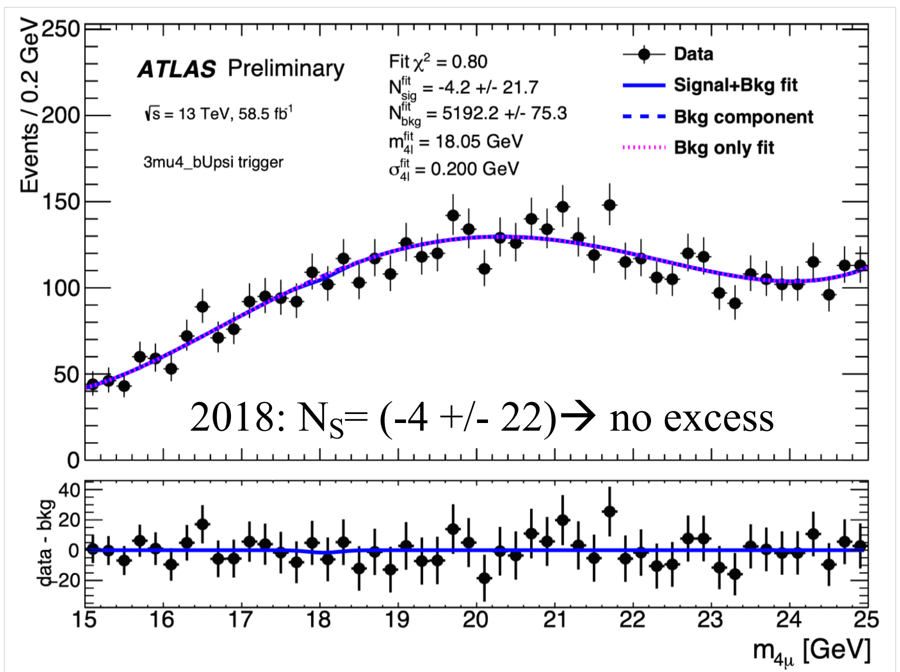

→ the combinatorial background is ~ 2.5 time larger per unit of integrated luminosity at 13 TeV w.r.t. 8 TeV

8 TeV data selected with the 3μ trigger

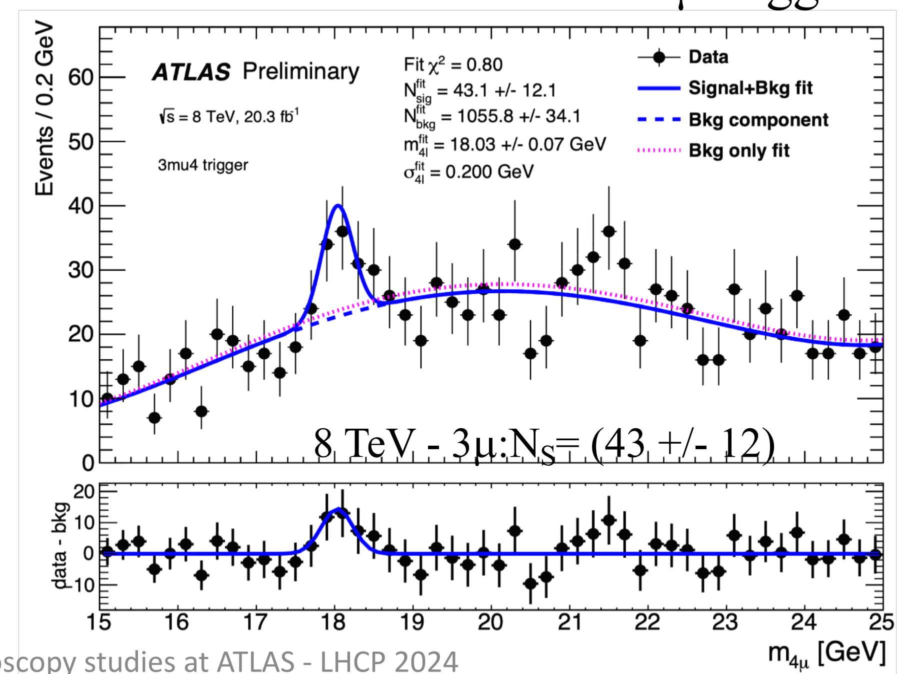

B.4 Signal interpretation and limit setting

→ observed upper limits at 95% CL and median expected (68-95)% CL intervals with a signal model of fixed $m_{4\mu}$(18GeV) and width (0.2GeV) and the CL_s construction

B.4 Signal interpretation and limit setting

→ observed upper limits at 95% CL and median expected (68-95)% CL intervals with a signal model of fixed $m_{4\mu}$(18GeV) and width (0.2GeV) and the CL_s construction

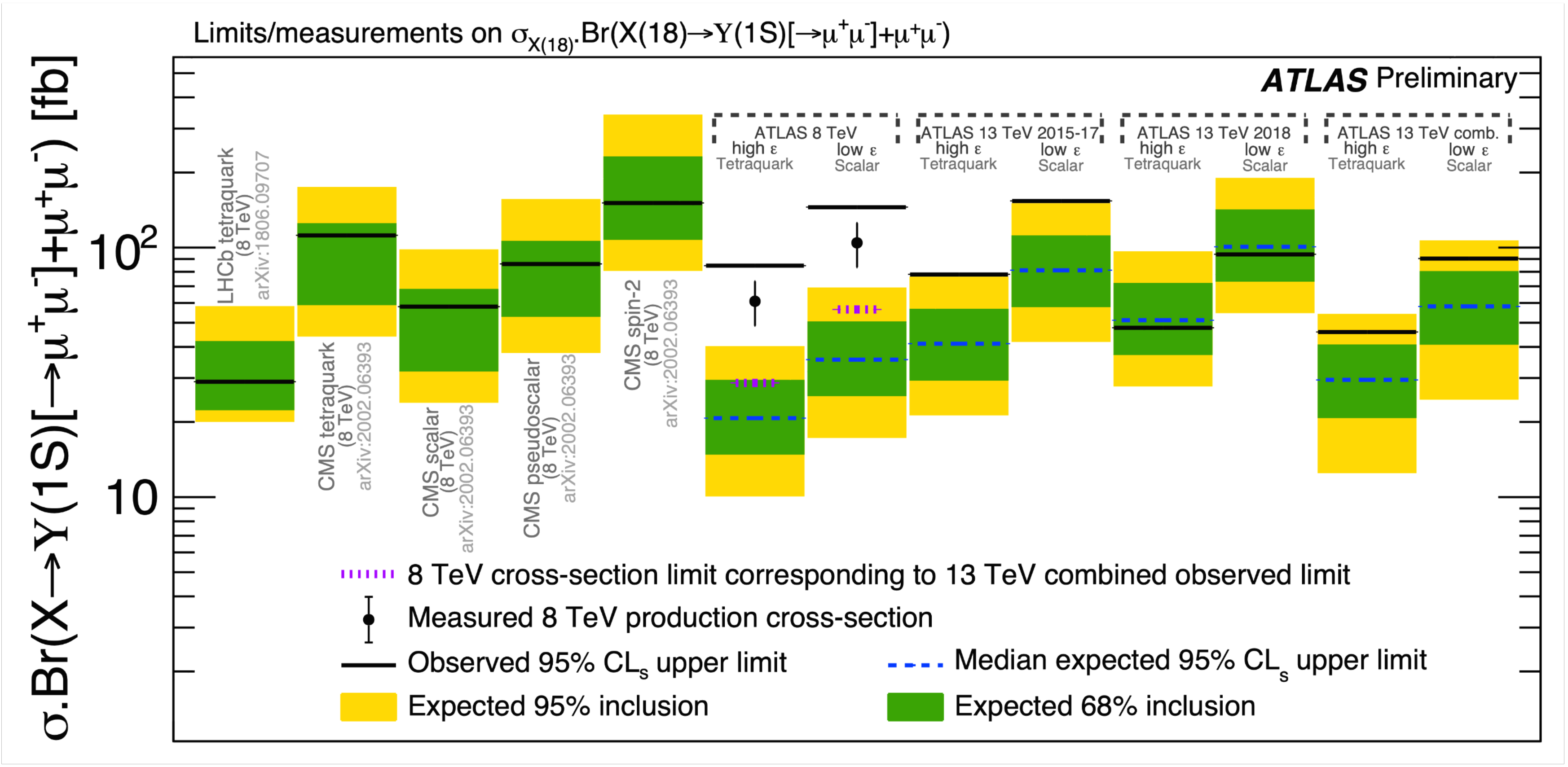

→ $(\sigma.BR)_{limit} \sim \varepsilon^{-1}$, therefore there is a large model-dependence of any interpretation (example of benchmark models with low/high ε are shown);

→ limits at different energies are not directly comparable;

→ picture is consistent with LHCB and CMS although they didn't observe excesses

C. Di-charmonium Events in the 4-muon final state:

Phys.Rev. Lett. 131, 151092 (2023)

C.1 “2-J/ψ →4μ” and “J/ψ +ψ(2s)→ 4μ” selection

Data sample: pp collisions at 13 TeV (2015-2018) corresponding to ~140 fb^{-1}

Trigger: requiring either 2 muons with invariant mass compatible with J/ψ or ψ(2s) (mass range [2.5,4.3] GeV) o 3 muons containing at least one such di-muon pair → efficiency would be ~72% for a TQ with m_X~7 GeV

C. Di-charmonium Events in the 4-muon final state:

Phys.Rev. Lett. 131, 151092 (2023)

C.1 "2-J/ψ → 4μ" and "J/ψ + ψ(2s) → 4μ" selection

Data sample: pp collisions at 13 TeV (2015-2018) corresponding to ~140 fb^{-1}

Trigger: requiring either 2 muons with invariant mass compatible with J/ψ or ψ(2s) (mass range [2.5,4.3] GeV) o 3 muons containing at least one such di-muon pair → efficiency would be ~72% for a TQ with m_X~7 GeV

Reconstruction: a) at least 4 muons (two opposite charge pairs) and fitted to common vertex; b) two pairs refitted with J/ψ or ψ(2s) mass; c) final mass $m_{4\mu}$

4μ vertex

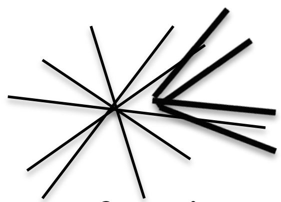

di-J/ψ or J/ψ +ψ(2s)

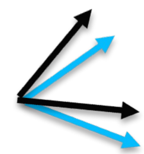

$m_{4\mu}$

→ dedicated cuts for signal (background) purification (suppression):

a) kinematics: $P_t^{(\mu)} > 4, 4, 3, 3$ GeV, $|\eta|<2.5$

b) mass constraints: 2.94 Gev $< m_{J/\psi} <$ 3.25 GeV, 3.56 Gev $< m_{\psi 2s} <$ 3.80 GeV, $m_{4\mu} <$ 11 Gev

c) vertex quality: $(\chi^2_{4\mu} / N_{4\mu}) < 3$

d) distances from primary vertex: $L_{xy}^{4\mu} < 0.2$ mm and both $L_{xy}^{2\mu} < 0.3$ mm

e) "distance" in phase space between 2- J/ψ or J/ψ +ψ(2s): $\Delta R = (\Delta\eta^2 + \Delta\phi^2)^{1/2} < 0.25$

→ mass resolution would be ~0.33% for a TQ with m_X~7 GeV

C.2 Background studies

C.2.1 Background sources and analysis strategy

1) non-prompt charmonium production from b-hadron decays
2) prompt single charmonium and non-resonant dimuon production
3) prompt double charmonium production in single/double parton scattering SPS/DPS

→ start with MC modelling and correct for discrepancies (e.g. kinematics) with data driven methods;

→ perform background analyses (validation and normalization) in dedicated control regions (CR) and then use transfer factors for yields in signal region (SR)

C.2 Background studies

C.2.1 Background sources and analysis strategy

1) non-prompt charmonium production from b-hadron decays
2) prompt single charmonium and non-resonant dimuon production
3) prompt double charmonium production in single/double parton scattering SPS/DPS

→ start with MC modelling and correct for discrepancies (e.g. kinematics) with data driven methods;

→ perform background analyses (validation and normalization) in dedicated control regions (CR) and then use transfer factors for yields in signal region (SR)

C.2.2 Non-prompt charmonium production b b-bar→2-$J/\psi + x$ or $J/\psi+\psi + x$

→ the decay vertex is displaced from primary pp interaction

→ the CR is obtained reversing the quality requirements on vertex $(\chi^2_{4\mu}/N_{4\mu})>6$ and both distances $L_{xy}^{2\mu} > 0.4$ mm

C.2 Background studies

C.2.1 Background sources and analysis strategy

1) non-prompt charmonium production from b-hadron decays
2) prompt single charmonium and non-resonant dimuon production
3) prompt double charmonium production in single/double parton scattering SPS/DPS

→ start with MC modelling and correct for discrepancies (e.g. kinematics) with data driven methods;

→ perform background analyses (validation and normalization) in dedicated control regions (CR) and then use transfer factors for yields in signal region (SR)

C.2.2 Non-prompt charmonium production b b-bar → 2-J/ψ + x or J/ψ+ψ + x

→ the decay vertex is displaced from primary pp interaction

→ the CR is obtained reversing the quality requirements on vertex $(\chi^2_{4\mu}/N_{4\mu})>6$ and both distances $L_{xy}^{2\mu} > 0.4$ mm

C.2.3 Prompt single charmonium and non-resonant 2−μ production (others)

→ at least one charmonium candidate containing random combination of "fake" muons

→ CR is obtained using charmonium for which one track is not tagged as muon

→ shape and normalization are obtained from events in charmonium mass side-bands $m_{J/\psi}$ (GeV) [2.60-2.80] + [3.34-3.50] and $m_{\psi(2s)}$ (GeV) [3.36-3.52] + [3.84-4.00]

C.2.4 Double charmonium production from SPS/DPS

→ MC simulation doesn't reproduce correctly data distributions for double charmonium (e.g di-J/ψ p_T, $\Delta\phi_{charm}$, $\Delta\eta_{charm}$, lowest muon p_T)

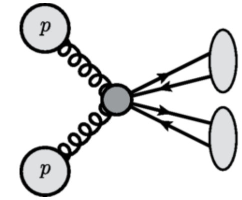

SPS

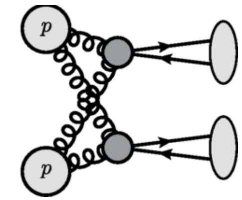

DPS

C.2.4 Double charmonium production from SPS/DPS

→ MC simulation doesn't reproduce correctly data distributions for double charmonium (e.g di-J/ψ p_T, $\Delta\phi_{charm}$, $\Delta\eta_{charm}$, lowest muon p_T)

→ need different dedicated control regions in $m_{4\mu}$ for tuning, without ΔR cut: a) SPS $m_{4\mu}$:[7.5-12] GeV b) DPS $m_{4\mu}$:[14-24.5] GeV

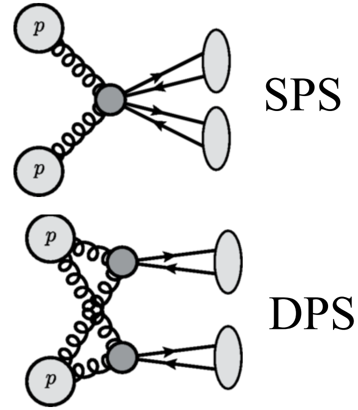

2-J/ψ

J/ψ +ψ(2s)

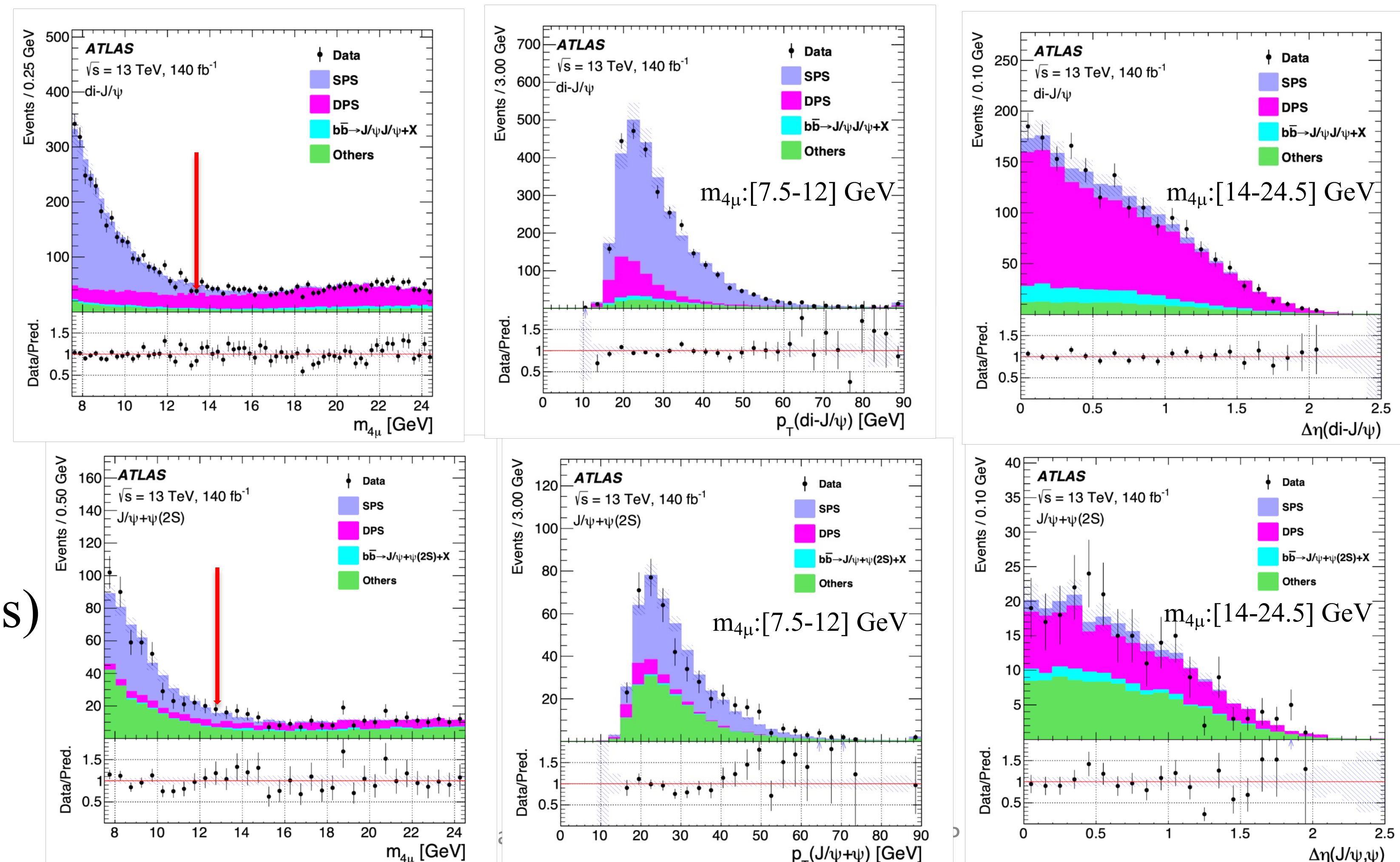

C.3 Analysis results

C.3.1 Final selection and fit

CR: $\Delta R > 0.25$
$m_{4\mu} < 11$ GeV

→ the background components give good description of the data

2-J/ψ sample

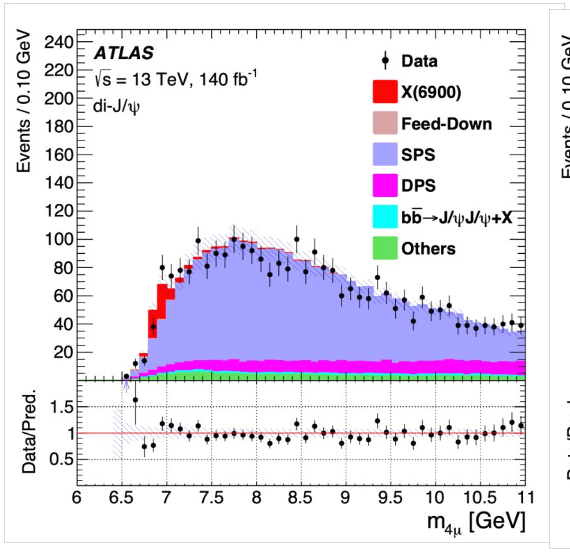

[J/ψ +ψ(2s)] sample

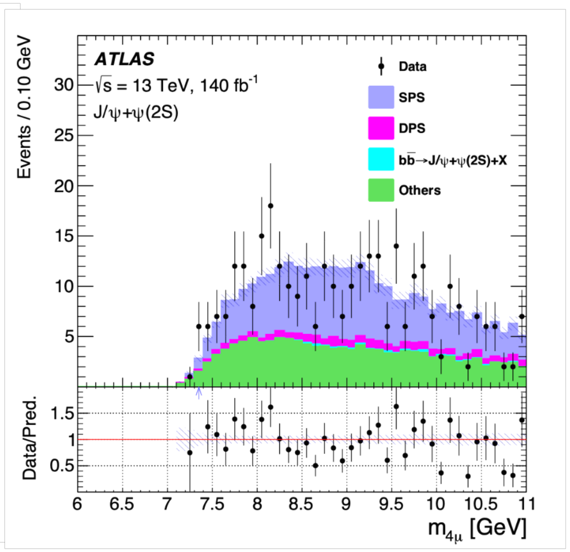

C.3 Analysis results

C.3.1 Final selection and fit

CR: $\Delta R > 0.25$
$m_{4\mu} < 11$ GeV

→ the background components give good description of the data

SR: $\Delta R < 0.25$
$m_{4\mu} < 9.2$ GeV

2-J/ψ sample

[J/ψ +ψ(2s)] sample

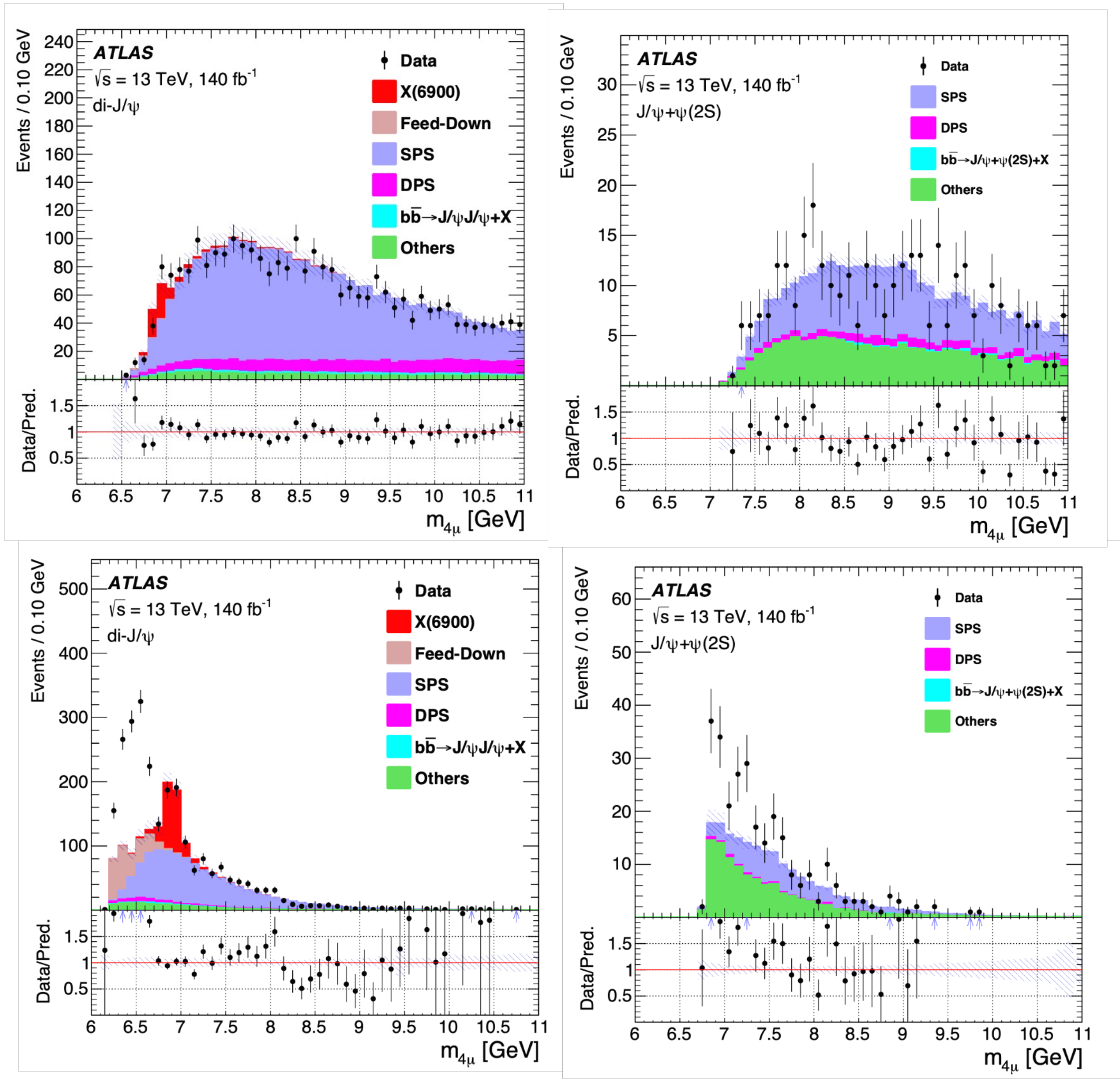

C.3 Analysis results

C.3.1 Final selection and fit

CR: $\Delta R > 0.25$

$m_{4\mu} < 11$ GeV

→ the background components give good description of the data

SR: $\Delta R < 0.25$

$m_{4\mu} < 9.2$ GeV

→ significant broad excess is observed over threshold (similar structures seen by CMS and the LHCb X(6900) "signal" is inserted)

2-J/ψ sample | [J/ψ +ψ(2s)] sample

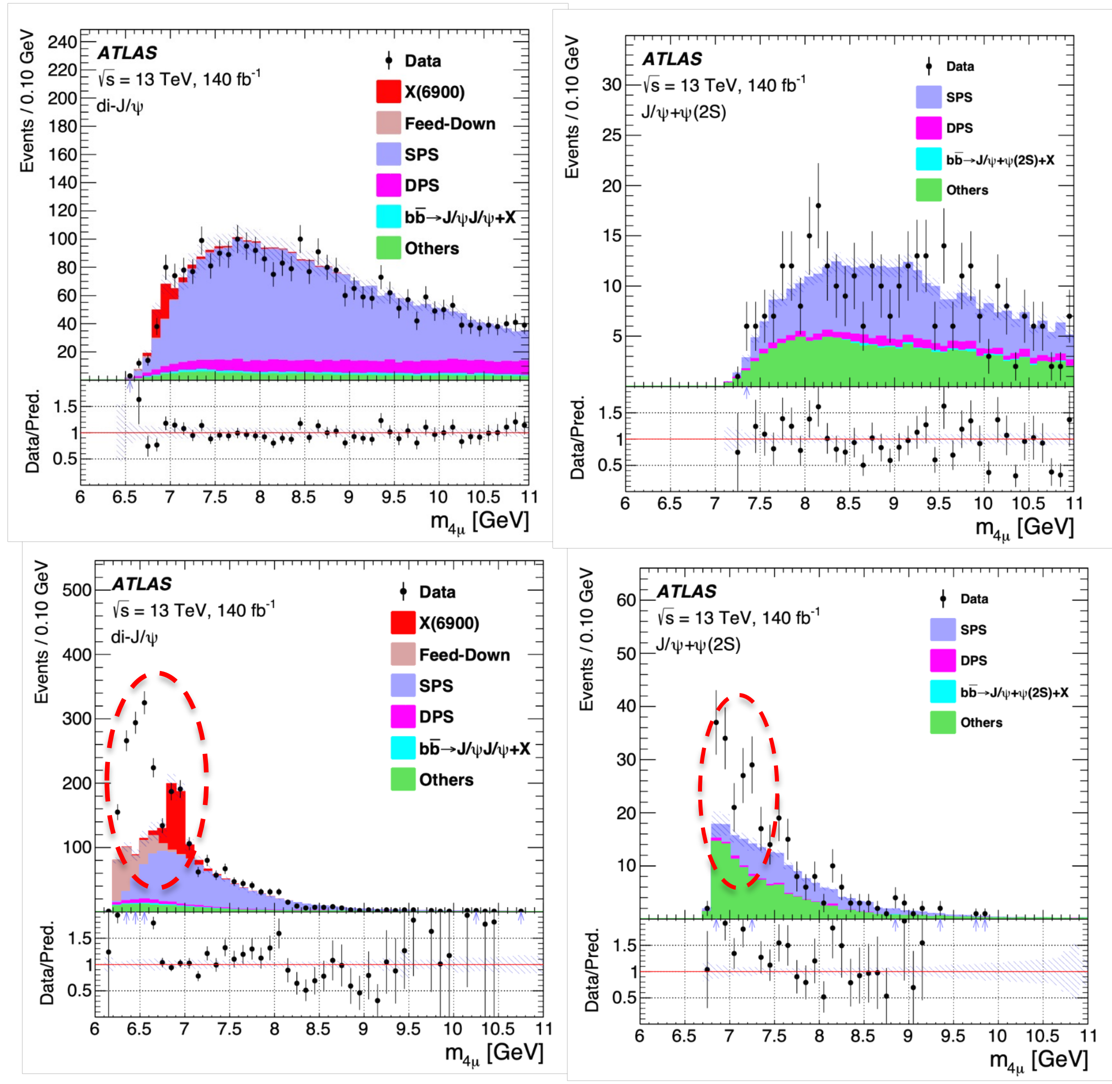

C.3 Analysis results

C.3.1 Final selection and fit

CR: $\Delta R > 0.25$

$m_{4\mu} < 11$ GeV

→ the background components give good description of the data

SR: $\Delta R < 0.25$

$m_{4\mu} < 9.2$ GeV

→ significant broad excess is observed over threshold (similar structures seen by CMS and the LHCb X(6900) "signal" is inserted)

2-J/ψ sample [J/ψ +ψ(2s)] sample

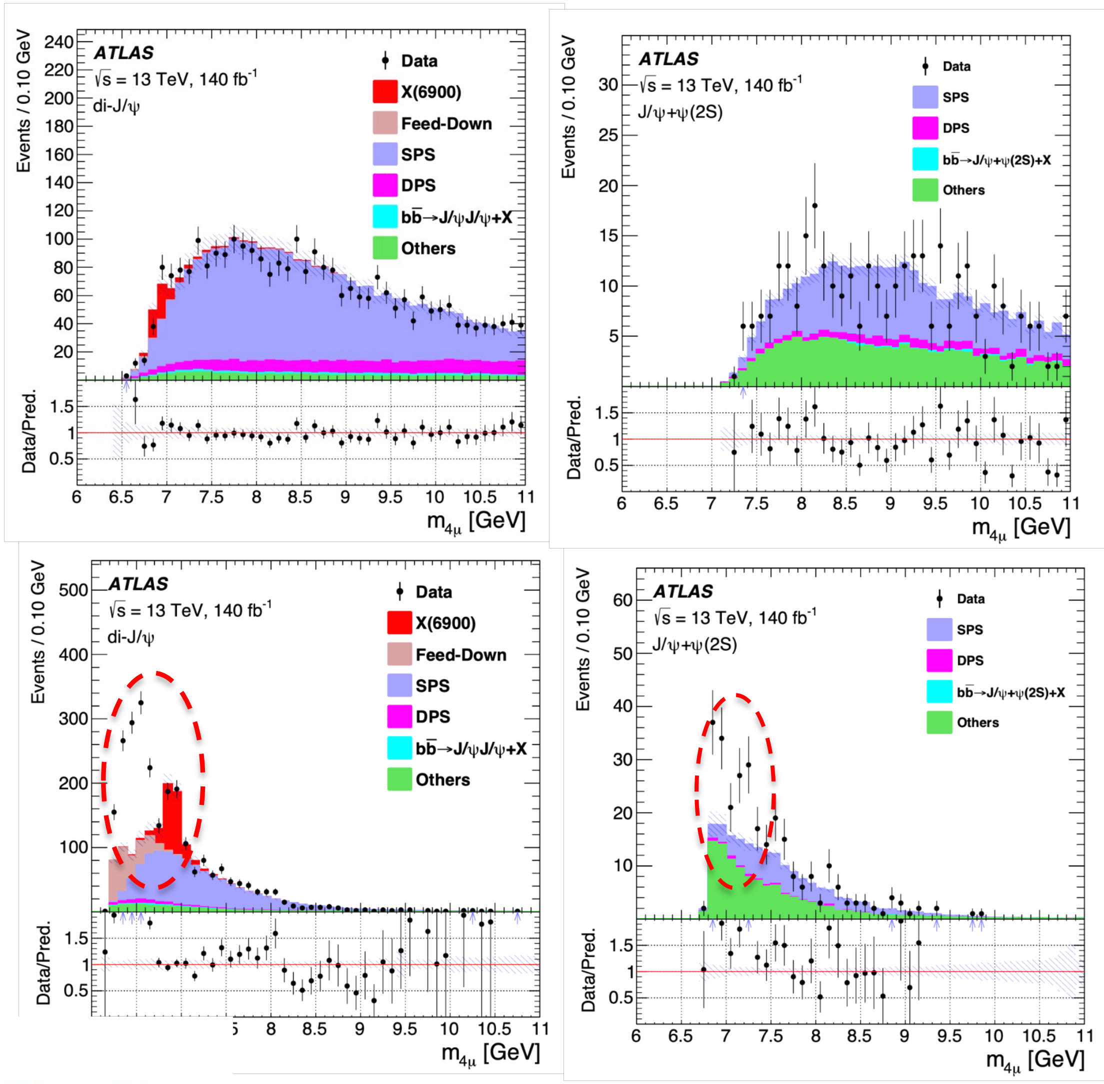

$$\mathcal{L} = \mathcal{L}_{SR}(\vec{\theta}, \vec{\lambda}) \cdot \mathcal{L}_{CR}(\vec{\theta}) \cdot \prod_{j=1}^{K} G(\theta'_j; \theta_j, \sigma_j),$$

→ λ_i parameters of interest

→ θ_i nuisance parameters with gaussian constraints from subsidiary measurements

Feed-down background

$\psi(2s) \rightarrow (X)' \rightarrow J/\psi + x$

$$N_{\rm fd} = \frac{\mathcal{B}' \epsilon'}{\mathcal{B}(\psi(2S) \rightarrow \mu\mu)\epsilon} N,$$

C.3.2 Analysis for the 2-J/ψ sample:

Model A

- n interfering S-wave BW, $z_i = |z_i|.e^{\phi i}$,
- phase space factor and resolution function

$$f_s(x) = \left| \sum_{i=0}^{2} \frac{z_i}{m_i^2 - x^2 - i m_i \Gamma_i(x)} \right|^2 \sqrt{1 - \frac{4m_{J/\psi}^2}{x^2}} \otimes R(\theta),$$

- fixed $|z_1|=1$ and other parameters free to vary
- number of resonances increased up to optimize the fit quality → n=3

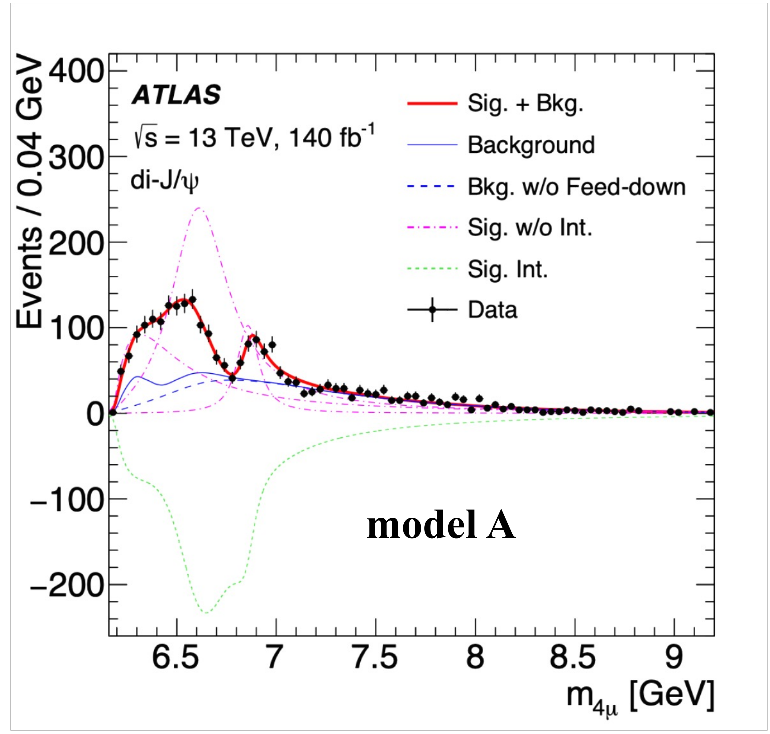

di-J/ψ	model A
m_0	$6.41 \pm 0.08^{+0.08}_{-0.03}$
Γ_0	$0.59 \pm 0.35^{+0.12}_{-0.20}$
m_1	$6.63 \pm 0.05^{+0.08}_{-0.01}$
Γ_1	$0.35 \pm 0.11^{+0.11}_{-0.04}$
m_2	$6.86 \pm 0.03^{+0.01}_{-0.02}$
Γ_2	$0.11 \pm 0.05^{+0.02}_{-0.01}$
$\Delta s/s$	$\pm 5.1\%^{+8.1\%}_{-8.9\%}$

m_i and Γ_i in GeV

C.3.2 Analysis for the 2-J/ψ sample:

Model A

- n interfering S-wave BW, $z_i = |z_i|.e^{\phi i}$,
- phase space factor and resolution function

$$f_s(x) = \left| \sum_{i=0}^{2} \frac{z_i}{m_i^2 - x^2 - i m_i \Gamma_i(x)} \right|^2 \sqrt{1 - \frac{4m_{J/\psi}^2}{x^2}} \otimes R(\theta),$$

- fixed $|z_1|=1$ and other parameters free to vary
- number of resonances increased up to optimize the fit quality → n=3

Model B

- two resonances (one interfering with SPS bkg)

$$f(x) = \left(\left| \frac{z_0}{m_0^2 - x^2 - i m_0 \Gamma_0(x)} + A(x) e^{i\phi} \right|^2 + \left| \frac{z_2}{m_2^2 - x^2 - i m_2 \Gamma_2(x)} \right|^2 \right) \sqrt{1 - \frac{4m_{J/\psi}^2}{x^2}} \otimes R(\theta)$$

di-J/ψ	model A	model B
m_0	$6.41 \pm 0.08^{+0.08}_{-0.03}$	$6.65 \pm 0.02^{+0.03}_{-0.02}$
Γ_0	$0.59 \pm 0.35^{+0.12}_{-0.20}$	$0.44 \pm 0.05^{+0.06}_{-0.05}$
m_1	$6.63 \pm 0.05^{+0.08}_{-0.01}$	—
Γ_1	$0.35 \pm 0.11^{+0.11}_{-0.04}$	—
m_2	$6.86 \pm 0.03^{+0.01}_{-0.02}$	$6.91 \pm 0.01 \pm 0.01$
Γ_2	$0.11 \pm 0.05^{+0.02}_{-0.01}$	$0.15 \pm 0.03 \pm 0.01$
$\Delta s/s$	$\pm 5.1\%^{+8.1\%}_{-8.9\%}$	—

m_i and Γ_i in GeV

consistent picture with the X(6900) seen by LHCb

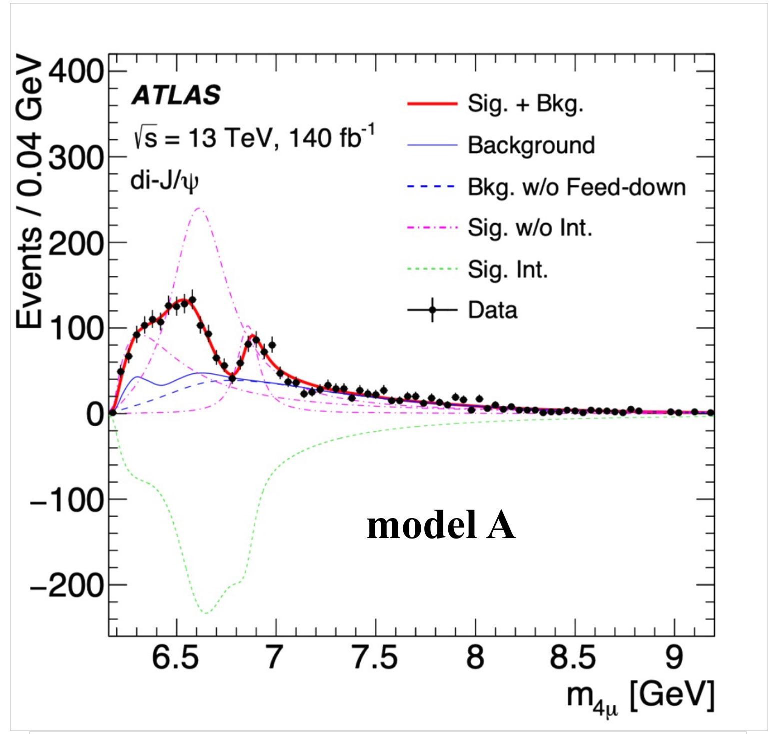

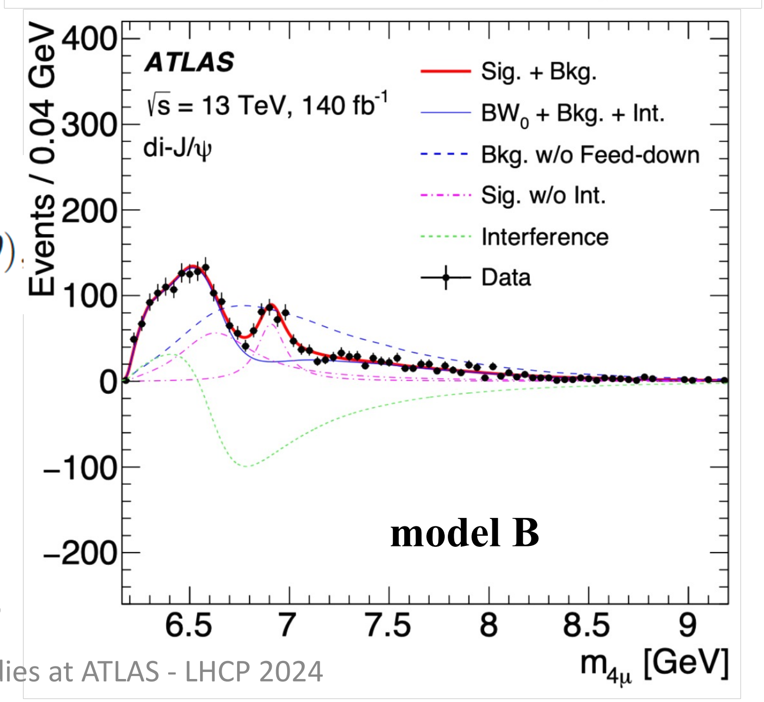

C.3.3 Analysis for the [J/ψ +ψ(2s)] sample

Model α: same (n=0,1,2) interfering resonances of 2-J/ψ sample and a fourth standalone one

$$f_s(x) = \left(\left| \sum_{i=0}^{2} \frac{z_i}{m_i^2 - x^2 - i m_i \Gamma_i(x)} \right|^2 + \left| \frac{z_3}{m_3^2 - x^2 - i m_3 \Gamma_3(x)} \right|^2 \right) \times \sqrt{1 - \left(\frac{m_{J/\psi} + m_{\psi(2S)}}{x} \right)^2} \otimes R(\theta)$$

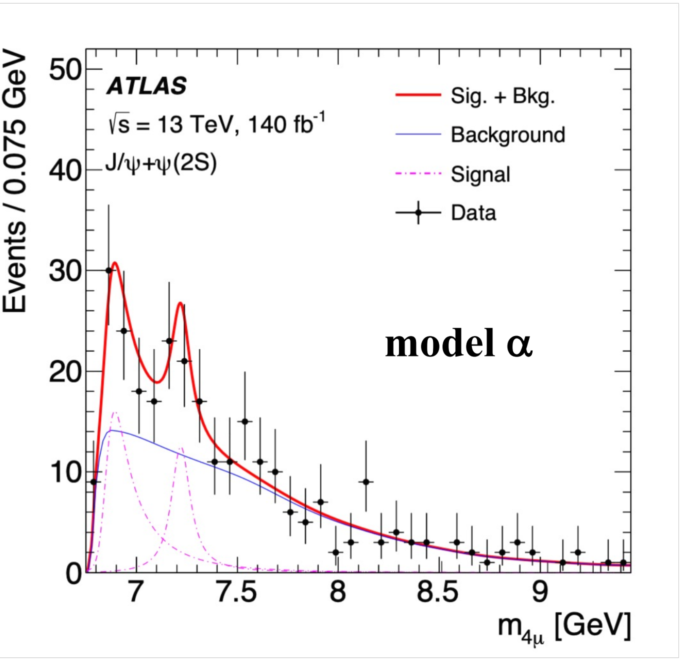

J/ψ+ψ(2S)	model α
m_3	$7.22 \pm 0.03^{+0.01}_{-0.04}$
Γ_3	$0.09 \pm 0.06^{+0.06}_{-0.05}$
$\Delta s/s$	$\pm 21\%^{+25\%}_{-15\%}$

m_i and Γ_i in GeV

C.3.3 Analysis for the [J/ψ +ψ(2s)] sample

Model α: same (n=0,1,2) interfering resonances of 2-J/ψ sample and a fourth standalone one

$$f_s(x) = \left(\left| \sum_{i=0}^{2} \frac{z_i}{m_i^2 - x^2 - i m_i \Gamma_i(x)} \right|^2 + \left| \frac{z_3}{m_3^2 - x^2 - i m_3 \Gamma_3(x)} \right|^2 \right) \times \sqrt{1 - \left(\frac{m_{J/\psi} + m_{\psi(2S)}}{x} \right)^2} \otimes R(\theta)$$

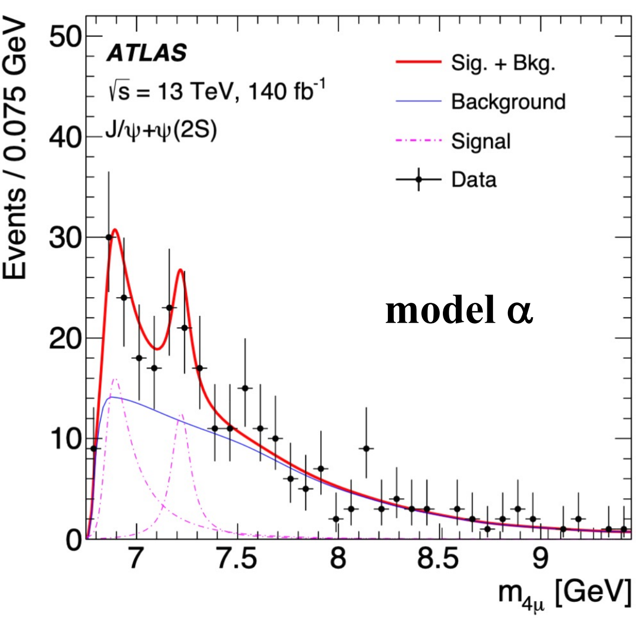

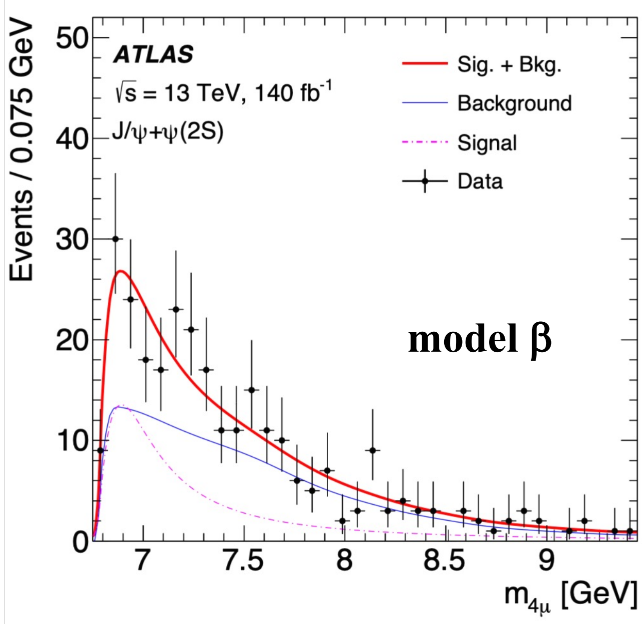

Model β:
single resonance
($z_0=z_1=z_2=0$)

J/ψ+ψ(2S)	model α	model β
m_3	$7.22 \pm 0.03^{+0.01}_{-0.04}$	$6.96 \pm 0.05 \pm 0.03$
Γ_3	$0.09 \pm 0.06^{+0.06}_{-0.05}$	$0.51 \pm 0.17^{+0.11}_{-0.10}$
$\Delta s/s$	$\pm 21\%^{+25\%}_{-15\%}$	$\pm 20\% \pm 12\%$

m_i and Γ_i in GeV

C.3.4 Systematic uncertainties

The relevant ones are those affecting the mass spectrum shape, and mainly:

X(6900) parameter	**Model A**		**Model α**	
Systematic	di-J/ψ		$J/\psi+\psi(2S)$	
Uncertainties (MeV)	m_2	Γ_2	m_3	Γ_3
Muon calibration	±6	±7	<1	±1
SPS model parameter	±7	±7	<1	
SPS di-charmonium p_T	±7	±8	<1	
Background MC sample size	±7	±8	±1	<1
Mass resolution	±4	−3	−1	$^{+2}_{-4}$
Fit bias	−13	+10	$^{+9}_{-10}$	$^{+50}_{-16}$
Shape inconsistency	<1		±4	±6
Transfer factor	—		±5	±23
Presence of 4th resonance	<1		—	
Feed-down	$^{+4}_{-1}$	$^{+6}_{-2}$	—	
Interference of 4th resonance	—		−32	−11
P and D-wave BW	+9	+19	<1	±1
ΔR and muon p_T requirements	$^{+3}_{-2}$	$^{+6}_{-4}$	$^{+1}_{-2}$	−2

C.3.4 Systematic uncertainties

The relevant ones are those affecting the mass spectrum shape, and mainly:

X(6900) parameter	Model A		Model α	
Systematic Uncertainties (MeV)	di-J/ψ		J/ψ+$\psi(2S)$	
	m_2	Γ_2	m_3	Γ_3
Muon calibration	±6	±7	<1	±1
SPS model parameter	±7	±7	<1	
SPS di-charmonium p_T	±7	±8	<1	
Background MC sample size	±7	±8	±1	<1
Mass resolution	±4	−3	−1	$^{+2}_{-4}$
Fit bias	−13	+10	$^{+9}_{-10}$	$^{+50}_{-16}$
Shape inconsistency	<1		±4	±6
Transfer factor	—		±5	±23
Presence of 4th resonance	<1		—	
Feed-down	$^{+4}_{-1}$	$^{+6}_{-2}$	—	
Interference of 4th resonance	—		−32	−11
P and D-wave BW	+9	+19	<1	±1
ΔR and muon p_T requirements	$^{+3}_{-2}$	$^{+6}_{-4}$	$^{+1}_{-2}$	−2

C.3.5 Significance and interpretation

→ significance from asymptotic formula on the profile likelihood

$$Z = \sqrt{2\ln[L(\hat{s},\hat{\theta})/L(0,\hat{\hat{\theta}})]}$$

C.3.4 Systematic uncertainties

The relevant ones are those affecting the mass spectrum shape, and mainly:

X(6900) parameter	**Model A**		**Model α**	
Systematic Uncertainties (MeV)	di-J/ψ		J/ψ+ψ(2S)	
	m_2	Γ_2	m_3	Γ_3
Muon calibration	±6	±7	<1	±1
SPS model parameter	±7	±7	<1	
SPS di-charmonium p_T	±7	±8	<1	
Background MC sample size	±7	±8	±1	<1
Mass resolution	±4	−3	−1	$^{+2}_{-4}$
Fit bias	−13	+10	$^{+9}_{-10}$	$^{+50}_{-16}$
Shape inconsistency	<1		±4	±6
Transfer factor	—		±5	±23
Presence of 4th resonance	<1		—	
Feed-down	$^{+4}_{-1}$	$^{+6}_{-2}$	—	
Interference of 4th resonance	—		−32	−11
P and D-wave BW	+9	+19	<1	±1
ΔR and muon p_T requirements	$^{+3}_{-2}$	$^{+6}_{-4}$	$^{+1}_{-2}$	−2

C.3.5 Significance and interpretation

→ significance from asymptotic formula on the profile likelihood

$$Z = \sqrt{2\ln[L(\hat{s},\hat{\theta})/L(0,\hat{\hat{\theta}})]}$$

For 2-J/ψ sample:

- for both models, the significance of all resonances far exceed 5σ and m_2 is consistent with LHCb X(6900);
- data cannot exclude that the low mass broad structure is related to other effects like T_{cccc} → (χ_{cJ} $\chi_{cJ'}$) → J/ψ J/ψ + x.

C.3.4 Systematic uncertainties

The relevant ones are those affecting the mass spectrum shape, and mainly:

X(6900) parameter	Model A		Model α	
Systematic Uncertainties (MeV)	di-J/ψ m_2	Γ_2	J/ψ+ψ(2S) m_3	Γ_3
Muon calibration	±6	±7	<1	±1
SPS model parameter	±7	±7	<1	
SPS di-charmonium p_T	±7	±8	<1	
Background MC sample size	±7	±8	±1	<1
Mass resolution	±4	−3	−1	$^{+2}_{-4}$
Fit bias	−13	+10	$^{+9}_{-10}$	$^{+50}_{-16}$
Shape inconsistency	<1		±4	±6
Transfer factor	—		±5	±23
Presence of 4th resonance	<1		—	
Feed-down	$^{+4}_{-1}$	$^{+6}_{-2}$	—	
Interference of 4th resonance	—		−32	−11
P and D-wave BW	+9	+19	<1	±1
ΔR and muon p_T requirements	$^{+3}_{-2}$	$^{+6}_{-4}$	$^{+1}_{-2}$	−2

C.3.5 Significance and interpretation

→ significance from asymptotic formula on the profile likelihood

$$Z = \sqrt{2\ln[L(\hat{s},\hat{\theta})/L(0,\hat{\hat{\theta}})]}$$

For 2-J/ψ sample:

- for both models, the significance of all resonances far exceed 5σ and m_2 is consistent with LHCb X(6900);
- data cannot exclude that the low mass broad structure is related to other effects like T_{cccc} → ($\chi_{cJ}\,\chi_{cJ'}$) → J/ψ J/ψ + x.

For [J/ψ + ψ(2s)] sample:

- the significances are 4.7σ (model α) and 4.3σ (model β);
- in the fit with model α, the significance of the second resonance alone is found to be 3.0σ

D) Conclusion

- ATLAS studied the four muon final states in pp collisions exploiting 21.3 fb^{-1} at 8 TeV and 139 fb^{-1} at 13 TeV

- An excess was observed at 8 TeV at $m_{4\mu}$~18 GeV in the finale state $\Upsilon(1s)+\mu^+\mu^- \rightarrow \mu^+\mu^- \mu^+\mu^-$. At 13 TeV, even though the sensitivity is reduced, the data do not support the 8 TeV signal.

D) Conclusion

- ATLAS studied the four muon final states in pp collisions exploiting 21.3 fb^{-1} at 8 TeV and 139 fb^{-1} at 13 TeV

- An excess was observed at 8 TeV at $m_{4\mu}$~18 GeV in the finale state $\Upsilon(1s)+\mu^+\mu^- \rightarrow \mu^+\mu^- \mu^+\mu^-$. At 13 TeV, even though the sensitivity is reduced, the data do not support the 8 TeV signal.

- At 13 TeV, in the final states "2-$J/\psi \rightarrow 4\mu$" and "$J/\psi + \psi(2s) \rightarrow 4\mu$", ATLAS confirmed the evidence of X(6900) already seen by LHCB and CMS; and similarly observed a significant excess over background above the kinematic production threshold which is compatible with the presence of new states decaying to 2-J/ψ

D) Conclusion

- ATLAS studied the four muon final states in pp collisions exploiting 21.3 fb^{-1} at 8 TeV and 139 fb^{-1} at 13 TeV

- An excess was observed at 8 TeV at $m_{4\mu}$~18 GeV in the finale state $\Upsilon(1s)+\mu^+\mu^- \rightarrow \mu^+\mu^- \mu^+\mu^-$. At 13 TeV, even though the sensitivity is reduced, the data do not support the 8 TeV signal.

- At 13 TeV, in the final states "2-J/ψ $\rightarrow$4μ" and "J/ψ +ψ(2s)$\rightarrow$ 4μ", ATLAS confirmed the evidence of X(6900) already seen by LHCB and CMS; and similarly observed a significant excess over background above the kinematic production threshold which is compatible with the presence of new states decaying to 2-J/ψ

- The analysis of the full LHC data sample will allow ATLAS to study other exotic channels for the heavy flavor spectroscopy

B.3.3 Di-Upsilon production as validation tool

Associated di-Υ(1s) production, both decaying into $\mu^+\mu^-$,can be used to study the effects on the various aspects of the analysis of the different conditions between 8 TeV and 13 TeV collisions, and it allows to check if this may cause substructures in $m_{4\mu}$

All data are analysed with identical selections as before → study the $m_{\mu\mu}$ of the OS doublet in the events (Υ(1s) + $\mu^+\mu^-$):

- at 8 TeV a structure is observed at (9.43+/-0.04) GeV, N_S= (25 +/- 9) corresponding to di-Υ(1s)
- at 13 TeV the yield of di-Υ(1s) is significantly reduced (40-60)% from extrapolation of 8 TeV data
- significance of di-Υ(1s) signal is reduced and the 2.5 increase of background/fb^{-1} is confirmed

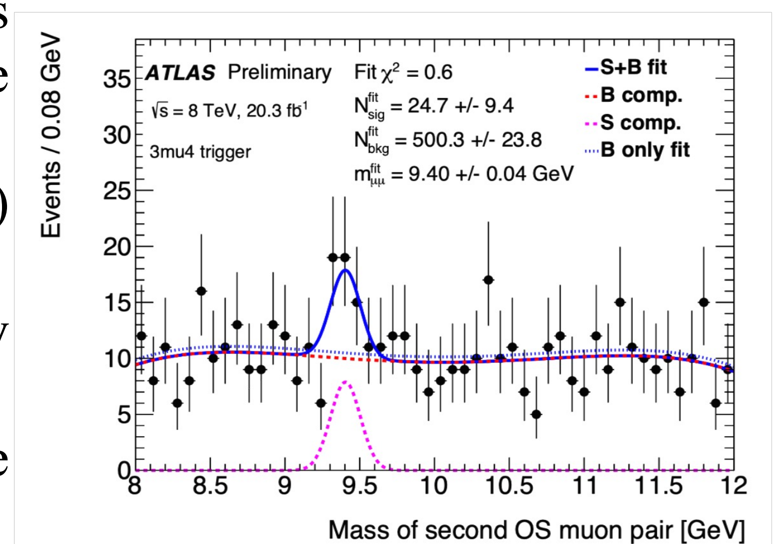

→ $m_{4\mu}$ pdf of di-Υ(1s) events is "uniform" above ~18.6 GeV, and cannot cause not for the 18 GeV excess itself

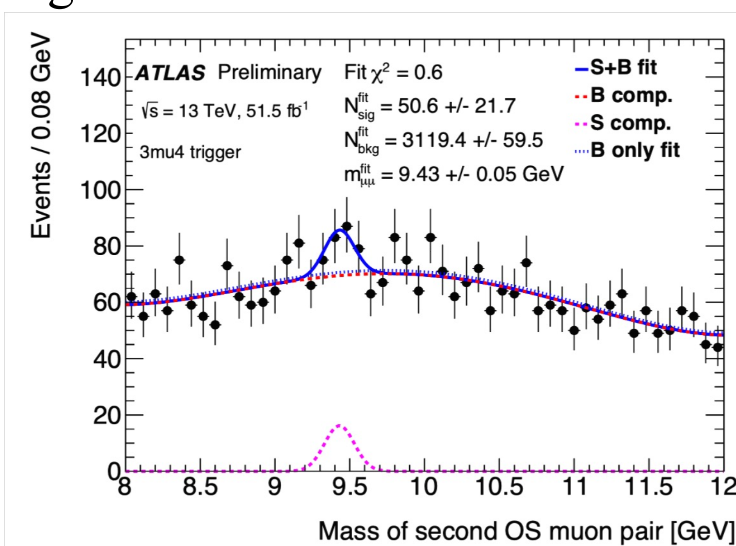

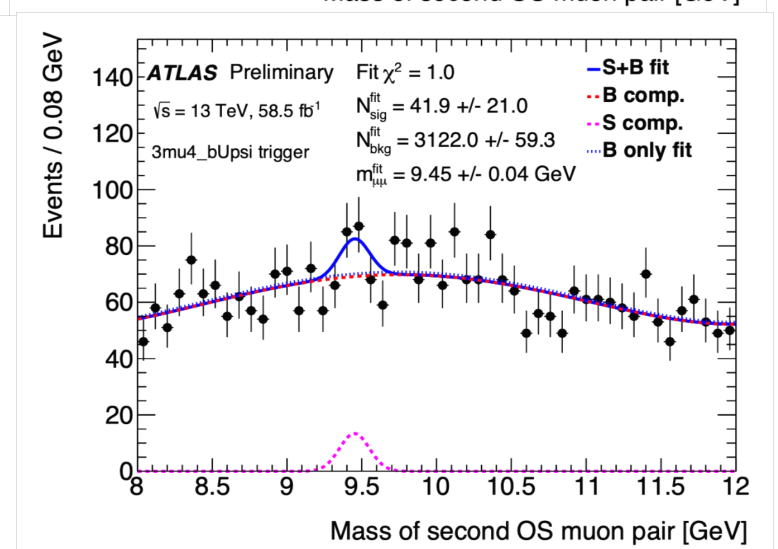

Reduce 8 TeV data with 3-μ trigger for comparison → important increase of background (~ 2 double events/fb^{-1})

Dataset	8 TeV		13 TeV	
Luminosity (fb^{-1})	20.3		51.5	58.5
Trigger	All triggers	3μ only	3μ only	3μ_bUpsi only
Four muons, ≥ 3 LowPt, $p_T > (4, 4, 3, 3)$ GeV	261,893	170,467	1,152,307	231,318
One $\Upsilon(1S)$ and $10 < m_{4\mu} < 50$ GeV	6,467	3,641 (179)	20,887 (406)	19,125 (327)
$\Upsilon(1S) + \mu^+\mu^-$	3,849	2,218 (109)	13,657 (265)	10,862 (186)
$\Upsilon(1S) + \mu^\pm\mu^\pm$	2,618	1,423 (70)	7,230 (140)	8,263 (141)